

運輸省港湾技術研究所

港湾技術研究所 報告

REPORT OF
THE PORT AND HARBOUR RESEARCH
INSTITUTE

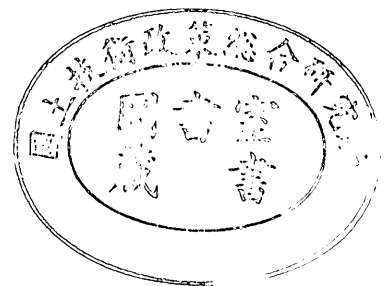
MINISTRY OF TRANSPORT

VOL. 8

NO. 4

DEC. 1969

NAGASE, YOKOSUKA, JAPAN



港湾技術研究所報告は第7巻第1号より年4回定期的に刊行する。ただし第1巻から第6巻および欧文編第1号から第15号までは下記のとおり不定期に刊行された。

報告の入手を希望する方は論文番号を明記して港湾技術研究所長に申し込んで下さい。

和文篇 (Japanese Edition)

- Vol. 1. No. 1 (1963)
- Vol. 2. Nos. 1~3 (1963~1964)
- Vol. 3. Nos. 1~7 (1964)
- Vol. 4. Nos. 1~11 (1965)
- Vol. 5. Nos. 1~15 (1966)
- Vol. 6. Nos. 1~8 (1967)

欧文篇 (English Edition)

- Report Nos. 1~15 (1963~1967)

The Report of the Port and Harbour Research Institute is published quarterly, either in Japanese or in occidental languages. The title and synopsis are given both in Japanese and in occidental languages.

The report prior to the seventh volume were published in two series in Japanese and English as listed above.

The copies of the Report are distributed to the agencies interested on the basis of mutual exchange of technical publication.

Inquiries relating to the Report should be addressed to the director of the Institute specifying the numbers of papers in concern.

港湾技術研究所報告 (REPORT OF P.H.R.I.)

第8巻 第4号 (Vol. 8, No. 4), 1969年12月 (Dec. 1969)

目 次 (CONTENTS)

1. The Problems of Density Current Part II.....Tokuichi HAMADA..... 3
(密度流の問題II.....浜田徳一)
2. Determination of Approximate Directional Spectra for Coastal Waves
..... Yoshimi SUZUKI..... 43
(沿岸波浪の近似的方向スペクトルの決定.....鈴木福実)
3. 圧密および膨張による飽和粘土のせん断強度の変化
..... 中瀬明男・小林正樹・勝野 克.....103
(Change in Undrained Shear Strength of Saturated Clays Through Consolidation
and Rebound.....Akio NAKASE, Masaki KOBAYASHI, Masaru KATSUNO)
4. 周辺補剛ばりを有する鉄筋コンクリートスラブの終局耐力について
..... 赤塚雄三・堀井修身・関 博.....145
(Ultimate Strength of Reinforced Concrete Slab with Boundary Frames Subjected to
a Concentrated LoadYuzo AKATSUKA, Osami HORIE, Hiroshi SEKI)
5. 総索引 (第7巻~第8巻)195
(Accumulative index (Vol. 7~Vol. 8))

| ページ | 欄 | 行 | 原文 | 訂正文 |
|-----|---|------------|--|---|
| 6 | 左 | 下 15 | 掘行 | 掘土 |
| 6 | 右 | 下 20 | 切断 | 考慮 |
| 7 | 右 | 上 1 | および車輪 | および車輪配置 |
| 13 | 右 | 下 20 | 掘さく | 掘さく |
| 33 | 左 | 下 13 | タイバー | タイバー |
| 33 | 左 | 下 9 | 鋪の装 | 鋪装の |
| 33 | 右 | 同上 | | 1:3 の配に天印をつけ |
| 34 | 左 | 図 24 の 2 倍 | 3 6 mm | 3 ~ 6 mm |
| 35 | 左 | 同上 | | みぞ幅 3-6mm, 深さ 25mm 程度 |
| 51 | 左 | 下 12 | 鉄網 | 鉄網 |
| 62 | 右 | 上 1 | 鉄網 | 鉄網 |
| 63 | 右 | 上 19 | 鉄網 | 鉄網 |
| 64 | 右 | 上 10 | 鉄網 | 鉄網 |
| 65 | 左 | 下 16 | 薄く必要 | 薄く敷く必要 |
| 66 | 右 | 上 4 | 付 採 | 付 近 |
| 71 | 左 | 下 14 | $h_2 = 5.0245 \sqrt{PN / \sigma_{ba}}$ | $h_2 = \frac{9.62 \times 10^{-3}}{K} \left(\frac{PN}{\sigma_{ba}} \right)^2$ |
| 71 | 左 | 下 10 | R : 鋼鉄入脚の半径 (cm) | K : 支持力係数 (kg/cm^2) |
| 71 | 右 | 上 15 | $EH^3 / 2 (1 - \mu^2) K$ | $EH^3 / 12 (1 - \mu^2) K$ |
| 71 | 右 | 上 15 | $40^3 / 2 (1 -$ | $40^3 / 12 (1 -$ |
| 78 | | 同上 | 等 | 3.5 |

2. Determination of Approximate Directional Spectra for Coastal Waves*

Yoshimi SUZUKI

Synopsis

The knowledge of the directional spectra for surface waves is essential to the problem of the wave generating mechanism by wind, and to the related problem of wave forecasting. It is important to the understanding of coastal phenomena, and consequently to the design of coastal works.

The author proposed a new method of determining the directional spectra of sea waves using the record of a wave meter and the record of a wave direction meter which can record X and Y component wave force acting on a bottom mounted sphere.

The accuracy of the method was investigated by means of simulated wave properties with directional spectra.

One set of actual data was analyzed by the method proposed herein, to obtain the approximate directional spectra. In addition, the value of C_D and C_M in the conventional wave force formula for the sphere were obtained as a function of component wave frequency.

* Partly reported in HEL 1-11, U.C. Berkeley, 1968.²¹⁾

2. 沿岸波浪の近似的方向スペクトルの決定

鈴木 禧 実

要 旨

風波の発生機構の解明，波浪の予報の問題において方向スペクトルを知ることは必須のことである。また，沿岸の諸現象および海岸における構造物の設計にも重要である。

著者は先に港湾技術研究所で開発された水圧式波高計およびストレーンゲージ式波向計の同時観測記録から，沿岸波浪の近似的方向スペクトルを算定する新しい方法を提案した。

この方法の近似の精度について，方向スペクトルをもつ波の諸元をシミュレーションにより発生させたデータにより調べ，波向きの算定精度は極めて良好なことを明らかにした。また，通常，水中の球に作用する波力の公式で用いられる C_D , C_M の値を周波数の関数として求めうることを示した。一例として酒田港における現地観測資料の解析を行ない近似的方向スペクトル，波向， C_D , C_M を求めた。

CONTENTS

| | |
|---|----|
| Synopsis | 43 |
| 1. Introduction | 47 |
| 2. Pseudo-integral Representation of Wave Properties | 47 |
| 3. Representation for Wave Force Acting on A Sphere in the Water | 49 |
| 4. Determination of the Directional Spectra for Surface Waves | 50 |
| 4.1 Cross-covariance functions | 51 |
| 4.2 Spectral densities | 54 |
| 4.3 Directional spectra for surface waves | 56 |
| 4.4 Simplification of the representation for the wave properties | 59 |
| 4.5 Application for the use of a pressure type wave meter | 62 |
| 5. Investigation of the Accuracy of the Method by Means of Simulated Wave Properties | 64 |
| 5.1 Simulation for sea surfaces having a directional spectral density by wave superposition | 64 |
| 5.2 Method of generating random phase | 66 |
| 5.3 Generating the simulated wave properties | 68 |
| 5.4 Accuracy of the method | 69 |
| 5.5 Characteristics of the simulated data | 75 |
| 6. Sample Calculation | 78 |
| 6.1 Method of observation | 78 |
| 6.2 Results of calculation | 79 |
| 7. Discussion | 83 |
| 8. Conclusion | 84 |
| Acknowledgements | 84 |
| Reference | 84 |
| List of Symbols | 86 |
| Appendix | 90 |

1. Introduction

In order to describe ocean waves in the generating area, characteristics of the irregularity of the sea surface waves including directional properties, must be measured. For design problems, wave direction is defined as the direction normal to the wave crest. The instantaneous wave direction, however, is different at any other space and time location. These conditions may be described by a directional spectrum which describes the distribution of wave energy with respect to direction and frequency. It is not easy to determine the directional spectrum either in the laboratory or in the ocean.

Four methods have been developed to obtain the directional spectrum for ocean waves. One is the method which makes use of a number of wave meters arranged in an array. Barber¹⁾ proposed this method and Cummins²⁾ (1959) used it in the experimental study in the U.S. Naval Taylor Model Basin. Barber³⁾ (1961) developed this method by studying the directional resolution properties. Mobarek⁴⁾ (1965) applied this method to the determination of the directional spectra for wind waves in a model basin. Another method makes use of stereo photographs taken from airplane (or shoreline). Cote⁵⁾ et. al. (1960) estimated the directional spectrum of sea waves by taking stereo photographs of the sea surface and measuring wave heights from these photographs at certain chosen grids point. Ijima et. al.⁶⁾ (1968) obtained the spectrum at KANAZAWA Coast by using the data taken by a stereo photographic camera. The third method is, so called, "Buoy method." Longuet-Higgins and Cartwright⁷⁾ (1961) succeeded in obtaining the directional spectra by measuring the heave, pitch and roll of buoy in the sea. Ewing⁸⁾ (1969) has obtained a sequence of ten records of the directional wave spectra from the motions of a floating buoy located in the North Atlantic. The fourth method was developed by Nagata⁹⁾ (1964). He measured the orbital motion in waves using an electromagnetic current meter; he studied the statistical properties of the motion, and proposed the method to obtain the directional spectra.

The purpose of the investigation reported herein is to propose a new method to determine the approximate directional spectra, using one set of a wave meter record together with the records of a specially developed wave direction meter.

2. Pseudo-integral Representation of Wave Properties

Wind generated waves can be thought of as being composed of an infinite number of waves with infinitesimal amplitudes each having its own frequency, f , traveling in its own particular direction, θ , and having random phase, Φ . Let the origin of the three space coordinates be on the sea floor. The vertical axis, z , is positive upward, while the two horizontal axes, x and y , are directed so that the x, y, z coordinate system is right-handed. Time will be denoted by t . Each wave has properties described by the small amplitude theory⁹⁾ (Linear theory).

Suppose that the sea surface, represented by $\hat{\eta}(x, y, t)$, is a Gaussian stationary stochastic process with parameters x, y and t then, after Pierson¹⁰⁾ (1954), it can be written as

$$\hat{\eta}(x, y, t) = \lim_{Q \rightarrow \infty} \lim_{\substack{M \rightarrow \infty \\ N \rightarrow \infty}} \sum_{m=1}^M \sum_{n=1}^N \sqrt{4p(f_m, \theta_n) \Delta f \Delta \theta} \\ \times \cos(k_m x \cos \theta_n + k_m y \sin \theta_n - 2\pi f_m t + \Phi_{mn}) \quad (1)$$

where $p(f_m, \theta_n)$ is the directional power spectral density for surface wave in the (f, θ) plane at $f=f_m$ and $\theta=\theta_n$. The values, f_m, θ_n and $\Delta f, \Delta \theta$ are defined as follows:

$$f=0, \frac{Q}{M}, \frac{2Q}{M}, \dots, \frac{MQ}{M} \quad (2)$$

$$\theta=0, \frac{2\pi}{N}, \frac{4\pi}{N}, \dots, \frac{2\pi N}{N} \quad (3)$$

$$\Delta f = \frac{Q}{M} \quad (4)$$

$$\Delta \theta = \frac{2\pi}{N} \quad (5)$$

f_m and θ_n denote the mid points of the intervals

$$\frac{(m-1)Q}{M} < f_m < \frac{mQ}{M} \quad (6)$$

and

$$\frac{2\pi(n-1)}{N} < \theta_n < \frac{2\pi n}{N} \quad (7)$$

Φ_{mn} is an independent random variable which is uniformly distributed over the interval $(0, 2\pi)$.

According to the small amplitude theory, a wave number, k_m , and a frequency, f_m , are interrelated by

$$(2\pi f_m)^2 = g k_m \tanh k_m d \quad (8)$$

Conventionally, Eq. (1) is often replaced by the following equation

$$\eta(x, y, t) = \int_0^\infty \int_0^{2\pi} \sqrt{4p(f, \theta) d\theta df} \cdot \cos(kx \cos \theta + ky \sin \theta - 2\pi ft + \Phi) \quad (9)$$

This represents a limiting form of Eq. (1). Equation (9), however, is neither an integral in the sense of analysis, nor a stochastic integral. This integral will be called a pseudo-integral.

Similarily, most wave properties can be written in terms of the pseudo-integral. The x and y component of horizontal water particle velocities at the space point (x, y, z) in the water depth of d are written as follows:

$$V_x(x, y, z; t) = 2 \int_0^\infty \int_0^{2\pi} \sqrt{p(f, \theta) d\theta df} \cdot (2\pi f) \cdot \cos \theta \cdot \frac{\cosh kz}{\sinh kd} \\ \times \cos(kx \cos \theta + ky \sin \theta - 2\pi ft + \Phi) \quad (10)$$

$$V_y(x, y, z; t) = 2 \int_0^\infty \int_0^{2\pi} \sqrt{p(f, \theta)} d\theta df \cdot (2\pi f) \cdot \sin \theta \frac{\cosh kz}{\sinh kd} \times \cos(kx \cos \theta + ky \sin \theta - 2\pi ft + \Phi) \quad (11)$$

Acceleration can be expressed as

$$A_x(x, y, z; t) = 2 \int_0^\infty \int_0^{2\pi} \sqrt{p(f, \theta)} d\theta df \cdot (2\pi f)^2 \cdot \cos \theta \left(\frac{\cosh kz}{\sinh kd} \right) \times \sin(kx \cos \theta + ky \sin \theta - 2\pi ft + \Phi) \quad (12)$$

$$A_y(x, y, z; t) = 2 \int_0^\infty \int_0^{2\pi} \sqrt{p(f, \theta)} d\theta df \cdot (2\pi f)^2 \cdot \sin \theta \left(\frac{\cosh kz}{\sinh kd} \right) \times \sin(kx \cos \theta + ky \sin \theta - 2\pi ft + \Phi) \quad (13)$$

Pressure fluctuation, η_p , can be described as

$$\eta_p(x, y, z; t) = 2 \int_0^\infty \int_0^{2\pi} \sqrt{p(f, \theta)} d\theta df \cdot \left(\frac{\cosh kz}{\cosh kd} \right) \cdot \omega \times \cos(kx \cos \theta + ky \sin \theta - 2\pi ft + \Phi) \quad (14)$$

where ω : specific weight of sea water.

3. Representation for Wave Force Acting on a Sphere in the Water

A statistical theory for the force on a submerged object, caused by ocean waves has been developed by Pierson¹¹⁾ (1963), Pierson and Holmes¹³⁾ (1965), Borgman¹³⁾ (1967), and Brown and Borgman¹⁴⁾ (1967). The basic underlying assumptions for the theory are that:

(a) The surface is a stationary, Gaussian stochastic process, and (b) the force is determined by the conventional engineering formula¹⁵⁾

$$F = C_1 V |V| + C_2 A_\sigma \quad (15)$$

where V is water particle velocity and A_σ is water particle acceleration. In this paper, it will be assumed that: (1) V and A_σ are two component Gaussian stochastic processes over the space and time coordinates, at a fixed space position, (x, y, z) , and instant in time, t , the random variables V and A_σ are independent with mean zero, and (2) the force formula given by Eq. (15) holds.

Then, the force equation for a sphere in the sea near the bottom can be as follows:

$$F = \frac{C_D \omega}{2g} \times (\pi r^2) \times V |V| + \frac{C_M \omega}{g} \left(\frac{4\pi r^3}{3} \right) \cdot A_\sigma \quad (16)$$

where r : radius of the sphere,
 C_D : drag coefficient,
 C_M : inertial coefficient,

g : acceleration of gravity,
and ω : specific weight of sea water.

In an approximate calculation, the term $V|V|$ in Eq. (15) can be assumed to be linearized by CV . According to Borgman¹⁶⁾ (1967), C is described in terms of the root-mean-square particle velocity, V_{rms} , as

$$C = V_{rms} \sqrt{\frac{8}{\pi}} \quad (17)$$

Then, Eq. (16) becomes

$$F \doteq \frac{C_D \omega}{2g} (\pi r^2) \cdot C \cdot V + \frac{C_M \omega}{g} \left(\frac{4}{3} \pi r^3 \right) A_\sigma \quad (18)$$

Further, let us assume that x and y component of the wave force can be expressed as

$$F_x \doteq \frac{C_D \omega}{2g} (\pi r^2) \cdot C \cdot V_x + \frac{C_M \omega}{g} \left(\frac{4}{3} \pi r^3 \right) A_x \quad (19)$$

and

$$F_y \doteq \frac{C_D \omega}{2g} (\pi r^2) \cdot C \cdot V_y + \frac{C_M \omega}{g} \left(\frac{4}{3} \pi r^3 \right) A_y \quad (20)$$

Inserting Eq. (10) through Eq. (13) into Eq. (19) and (20), the pseudo-integral representation for the components of the wave force are obtained as

$$\begin{aligned} F_x(x, y, z; t) &\doteq \frac{C_D \omega}{2g} (\pi r^2) \cdot C \cdot 2 \int_0^\infty \int_0^{2\pi} \sqrt{p(f, \theta)} d\theta df \cdot (2\pi f) \left(\frac{\cosh kz}{\sinh kd} \right) \\ &\quad \times \cos \theta \cdot \cos(kx \cos \theta + ky \sin \theta - 2\pi ft + \Phi) \\ &\quad + \frac{C_M \omega}{g} \left(\frac{4}{3} \pi r^3 \right) \cdot 2 \int_0^\infty \int_0^{2\pi} \sqrt{p(f, \theta)} d\theta df \cdot (2\pi f)^2 \left(\frac{\cosh kz}{\sinh kd} \right) \\ &\quad \times \cos \theta \sin(kx \cos \theta + ky \sin \theta - 2\pi ft + \Phi) \end{aligned} \quad (21)$$

$$\begin{aligned} F_y(x, y, z; t) &\doteq \frac{C_D \omega}{2g} (\pi r^2) \cdot C \cdot 2 \int_0^\infty \int_0^{2\pi} \sqrt{p(f, \theta)} d\theta df \cdot (2\pi f) \left(\frac{\cosh kz}{\sinh kd} \right) \\ &\quad \times \sin \theta \cdot \cos(kx \cos \theta + ky \sin \theta - 2\pi ft + \Phi) \\ &\quad + \frac{C_M \omega}{g} \left(\frac{4}{3} \pi r^3 \right) \cdot 2 \int_0^\infty \int_0^{2\pi} \sqrt{p(f, \theta)} d\theta df \cdot (2\pi f)^2 \left(\frac{\cosh kz}{\sinh kd} \right) \\ &\quad \times \sin \theta \sin(kx \cos \theta + ky \sin \theta - 2\pi ft + \Phi) \end{aligned} \quad (22)$$

4. Determination of the Directional Spectra for Surface Waves

Suppose we have the following data:

(a) $\eta(x, y, t)$; a record of the sea surface variation at a space point (x, y) with respect to time t ,

(b) $F_x(x, y, z, t)$; a record of x component wave force acting on a sphere at a space point, (x_1, y_1, z_1) , with respect to time, t , and

(c) $F_y(x, y, z, t)$; a record of y component wave force acting on a sphere at a space point, (x_2, y_2, z_2) , with respect to time, t .

The problem to be solved is how to determine the approximate two-dimensional spectra using the records.

Since these data are considered to be one realization of a random stochastic process which is stationary and has a zero mean, cross-spectrum densities in terms of the directional spectral density can be determined by taking the Fourier transform of cross covariance functions for the data.

The calculations for the cross-covariance function and the cross-spectrum density for the wave properties will be discussed first and the method of the determination of the approximate directional spectra will be discussed next in this section.

4.1 Cross-covariance functions

Let $X_1(x, y, t)$ and $X_2(x, y, t)$ be two real Gaussian stationary stochastic processes with parameters x, y and t , and with zero mean, then, the cross-covariance function, $C_{x_1x_2}$, for X_1 and X_2 is defined as

$$\begin{aligned} C_{x_1x_2}(g, h, \tau) &= \text{COV}[X_1(x, y, t), X_2(x+g, y+h, t+\tau)] \\ &= E[X_1(x, y, t)X_2(x+g, y+h, t+\tau)] \end{aligned} \quad (23)$$

where g is the lag in x , h the lag in y , and τ the lag in t . $E[]$ denotes the expectation operation.

Using Eq. (9), covariance function for η , $C_{\eta\eta}$, can be obtained as follows:

$$C_{\eta\eta}(g, h, \tau) = E[\eta(x, y, t)\eta(x+g, y+h, t+\tau)] \quad (24)$$

Let $C_{\eta\eta(mn)}(g, h, \tau)$ be the covariance of the (m, n) -th term in the sum in Eq. (1) with itself lagged. Then referring to Eq. (1),

$$\begin{aligned} C_{\eta\eta(mn)}(g, h, \tau) &= E[4p(f_m, \theta_n)\Delta f \Delta \theta \cos(k_mx \cos \theta_n + k_my \sin \theta_n \\ &\quad - 2\pi f_mt + \Phi_{mn}) \cdot \cos\{k_m(x+g) \cos \theta_n + k_m(y+h) \sin \theta_n - 2\pi f_m(t+\tau) + \Phi_{mn}\}] \\ &= E[4p(f_m, \theta) \Delta f \Delta \theta \cdot \frac{1}{2} \{\cos(k_mg \cos \theta_n + k_mh \sin \theta_n - 2\pi f_m\tau) \\ &\quad + \cos(k_m(2x+g) \cos \theta_n + k_m(2y+h) \sin \theta_n - 2\pi f_m(2t+\tau) + 2\Phi_{mn})\}] \end{aligned} \quad (25)$$

Since the expectation of cosine term including random phase, Φ is zero,

$$E[\cos(\varphi + \Phi)] = \frac{1}{2\pi} \int_0^{2\pi} \cos(\varphi + \Phi) d\Phi = 0 \quad (26)$$

then, the second term in Eq. (25) is zero. Eq. (25) becomes

$$C_{\eta\eta(mn)}(g, h, \tau) = 2p(f_m, \theta_n) \cos(k_mg \cos \theta_n + k_mh \sin \theta_n - 2\pi f_m\tau) \quad (27)$$

Since the cross products are zero by the assumption of independence, the covariance function for η is obtained by taking summation of Eq. (27) with respect to f and θ , and in the limit, $C_{\eta\eta}$ becomes

$$C_{\eta\eta}(g, h, \tau) = \int_0^\infty \int_0^{2\pi} 2p(f, \theta) \cos(kg \cos \theta + kh \sin \theta - 2\pi f \tau) d\theta df \quad (28)$$

Similary, covariance functions for the wave properties are obtained as follows:

Let
$$K_D = C_D \frac{\omega}{2g} \pi r^3 C$$

$$K_M = C_M \frac{\omega}{g} \frac{4}{3} \pi r^3$$

so that

$$F_x = K_D V_x + K_M A_x$$

$$F_y = K_D V_y + K_M A_y$$

$$\begin{aligned} C_{\eta F_x}(g, h, \tau) &= \text{COV} [\eta(x, y, t), F_x(x+g, y+h, t+\tau)] \\ &= \text{COV} [\eta(x, y, t), K_D V_x + K_M A_x] \\ &= E[\eta(x, y, t) K_D V_x(x+g, y+h, t+\tau)] \\ &\quad + E[\eta(x, y, t) K_M A_x(x+g, y+h, t+\tau)] \\ &= E \left[2 \int_0^\infty \int_0^{2\pi} \sqrt{p(f, \theta)} d\theta df \cos(kx \cos \theta + ky \sin \theta - 2\pi f t + \Phi) \right. \\ &\quad \times 2 \int_0^\infty \int_0^{2\pi} \sqrt{p(f, \theta)} d\theta df \cdot K_D \cdot 2\pi f \cdot \frac{\cosh kz}{\sinh kd} \cos \theta \\ &\quad \times \cos \{k(x+g) \cos \theta + k(y+h) \sin \theta - 2\pi f(t+\tau) + \Phi\} \Big] \\ &\quad + E \left[2 \int_0^\infty \int_0^{2\pi} \sqrt{p(f, \theta)} d\theta df \cos(kx \cos \theta + ky \sin \theta - 2\pi f t + \Phi) \right. \\ &\quad \times 2 \int_0^\infty \int_0^{2\pi} \sqrt{p(f, \theta)} d\theta df \cdot K_M \cdot (2\pi f)^2 \left(\frac{\cosh kz}{\sinh kd} \right) \cdot \cos \theta \\ &\quad \times \sin \{k(x+g) \cos \theta + k(y+h) \sin \theta - 2\pi f(t+\tau) + \Phi\} \Big] \\ &= 2 \int_0^\infty \int_0^{2\pi} p(f, \theta) K_D 2\pi f \frac{\cosh kz}{\sinh kd} \cos \theta \\ &\quad \times \cos(kg \cos \theta + kh \sin \theta - 2\pi f \tau) d\theta df \\ &\quad + 2 \int_0^\infty \int_0^{2\pi} p(f, \theta) K_M (2\pi f)^2 \left(\frac{\cosh kz}{\sinh kd} \right) \cos \theta \\ &\quad \times \sin(kg \cos \theta + kh \sin \theta - 2\pi f \tau) d\theta df \end{aligned}$$

Let

$$C''_D = K_D \frac{\cosh kz}{\sinh kd} (2\pi f) \quad (29)$$

$$C''_M = K_M \left(\frac{\cosh kz}{\sinh kd} \right) (2\pi f)^2 \quad (30)$$

then

$$\begin{aligned}
 C_{\eta F_x}(g, h, \tau) &= \int_0^\infty \int_0^{2\pi} C_D'' \cdot 2p(f, \theta) \cos \theta \\
 &\quad \times \cos(kg \cos \theta + kh \sin \theta - 2\pi f \tau) d\theta df \\
 &\quad + \int_0^\infty \int_0^{2\pi} C_M'' \cdot 2p(f, \theta) \cos \theta \\
 &\quad \times \sin(kg \cos \theta + kh \sin \theta - 2\pi f \tau) d\theta df
 \end{aligned} \tag{31}$$

$$\begin{aligned}
 C_{\eta F_y}(g, h, \tau) &= \int_0^\infty \int_0^{2\pi} C_D'' \cdot 2p(f, \theta) \sin \theta \\
 &\quad \times \cos(kg \cos \theta + kh \sin \theta - 2\pi f \tau) d\theta df \\
 &\quad + \int_0^\infty \int_0^{2\pi} C_M'' \cdot 2p(f, \theta) \sin \theta \\
 &\quad \times \sin(kg \cos \theta + kh \sin \theta - 2\pi f \tau) d\theta df
 \end{aligned} \tag{32}$$

$$\begin{aligned}
 C_{F_x F_x}(g, h, \tau) &= \text{COV}[F_x(x, y, t), F_x(x+g, y+h, t+\tau)] \\
 &= E[F_x(x, y, t)F_x(x+g, y+h, t+\tau)] \\
 &= E\{[K_D V_x(x, y, t) + K_M A_x(x, y, t)] \\
 &\quad \times [K_D V_x(x+g, y+h, t+\tau) + K_M A_x(x+g, y+h, t+\tau)]\} \\
 &= K_D^2 E[V_x(x, y, t)V_x(x+g, y+h, t+\tau)] \\
 &\quad + K_M^2 E[A_x(x, y, t)A_x(x+g, y+h, t+\tau)] \\
 &\quad + K_D K_M E[A_x(x, y, t)V_x(x+g, y+h, t+\tau)] \\
 &\quad + K_M K_D E[V_x(x, y, t)A_x(x+g, y+h, t+\tau)]
 \end{aligned} \tag{33}$$

Since

$$\begin{aligned}
 &E[A_x(x, y, t)V_x(x+g, y+h, t+\tau)] \\
 &= -E[V_x(x, y, t)A_x(x+g, y+h, t+\tau)]
 \end{aligned}$$

the last two terms in Eq. (33) are cancelled.

$$\begin{aligned}
 C_{F_x F_x}(g, h, \tau) &= K_D^2 E \left[\left\{ 2 \int_0^\infty \int_0^{2\pi} \sqrt{p(f, \theta)} d\theta df \cdot (2\pi f) \cdot \frac{\cosh kz}{\sinh kd} \cos \theta \right. \right. \\
 &\quad \times \cos(kx \cos \theta + ky \sin \theta - 2\pi f t + \Phi) \left. \right\} \\
 &\quad \times \left\{ 2 \int_0^\infty \int_0^{2\pi} \sqrt{P(f, \theta)} d\theta df \cdot (2\pi f) \cdot \frac{\cosh kz}{\sinh kd} \cos \theta \right. \\
 &\quad \times \cos(k(x+g) \cos \theta + k(y+h) \sin \theta - 2\pi f(t+\tau) + \Phi) \left. \right\} \Big] \\
 &\quad + \text{inertia term} \\
 &= 2 \int_0^\infty \int_0^{2\pi} (C_D''^2 + C_M''^2) P(f, \theta) \cos^2 \theta \\
 &\quad \times \cos(kg \cos \theta + kh \sin \theta - 2\pi f \tau) d\theta df
 \end{aligned} \tag{34}$$

Similarly $C_{F_y F_y}$ and $C_{F_x F_y}$ are obtained as follows.

$$C_{F_y F_y}(g, h, \tau) = 2 \int_0^\infty \int_0^{2\pi} (C_D'^2 + C_M'^2) p(f, \theta) \sin^2 \theta \times \cos(kg \cos \theta + kh \sin \theta - 2\pi f \tau) d\theta df \quad (35)$$

$$C_{F_x F_y}(g, h, \tau) = 2 \int_0^\infty \int_0^{2\pi} (C_D'^2 + C_M'^2) p(f, \theta) \sin \theta \cos \theta \times \cos(kg \cos \theta + kh \sin \theta - 2\pi f \tau) d\theta df \quad (36)$$

4.2 Spectral densities; Auto-, Co-, and Quadrature-spectrum

For the one-dimensional and real Gaussian stationary processes $X_1(t)$ and $X_2(t)$, covariance function for them, $C_{x_1 x_2}(\tau)$, is formulated by cross-spectral density, $P_{x_1 x_2}(f)$, as

$$C_{x_1 x_2}(\tau) = \int_{-\infty}^\infty P_{x_1 x_2}(f) e^{-i2\pi f \tau} df \quad (37)$$

$P_{x_1 x_2}(f)$ is represented by real and imaginary part as

$$P_{x_1 x_2}(f) = co(f) - iq(f) \quad (38)$$

$co(f)$ is called co-spectral density and $q(f)$ is called quadrature spectral density. Using Eq. (38), $C_{x_1 x_2}(\tau)$ is formulated in terms of $co(f)$ and $q(f)$ as follows.

$$\begin{aligned} C_{x_1 x_2}(\tau) &= \int_{-\infty}^\infty P_{x_1 x_2}(f) e^{i2\pi f \tau} df \\ &= \int_{-\infty}^\infty [co(f) - iq(f)] [\cos 2\pi f \tau + i \sin 2\pi f \tau] df \\ &= \int_{-\infty}^\infty co(f) \cos 2\pi f \tau df + \int_{-\infty}^\infty q(f) \sin 2\pi f \tau df \\ &\quad + i \int_{-\infty}^\infty co(f) \sin 2\pi f \tau df - i \int_{-\infty}^\infty q(f) \cos 2\pi f \tau df \end{aligned} \quad (39)$$

The last two integrals are zero since the integrands are odd functions of f . Since the remaining integrands are even, integrand may be restricted to $(0 \sim \infty)$.

$$C_{x_1 x_2}(\tau) = 2 \int_0^\infty co(f) \cos 2\pi f \tau df + 2 \int_0^\infty q(f) \sin 2\pi f \tau df \quad (40)$$

Using trigonometric identity, Eq. (28) can be written as

$$\begin{aligned} C_{\eta\eta}(g, h, \tau) &= \int_0^\infty \int_0^{2\pi} 2p(f, \theta) \cos(kg \cos \theta + kh \sin \theta - 2\pi f \tau) d\theta df \\ &= 2 \int_0^\infty \left\{ \int_0^{2\pi} p(f, \theta) \cos(kg \cos \theta + kh \sin \theta) d\theta \right\} \cos 2\pi f \tau df \\ &\quad + 2 \int_0^\infty \left\{ \int_0^{2\pi} p(f, \theta) \sin(kg \cos \theta + kh \sin \theta) d\theta \right\} \sin 2\pi f \tau df \end{aligned} \quad (41)$$

Comparing Eq. (41) with Eq. (40), co-spectrum and quadrature spectrum for

Determination of Approximate Directional Spectra for Coastal Waves

$\eta(x, y, t)$ can be obtained as a function of frequency in terms of $p(f, \theta)$ as follows:

$$\left. \begin{aligned} co_{\eta\eta}(f) &= \int_0^{2\pi} p(f, \theta) \cos(kg \cos \theta + kh \sin \theta) d\theta \\ q_{\eta\eta}(f) &= \int_0^{2\pi} p(f, \theta) \sin(kg \cos \theta + kh \sin \theta) d\theta \end{aligned} \right\} \quad (42)$$

Therefore, the cross- spectral density for η , $P_{\eta\eta}$, is obtained as

$$\begin{aligned} P_{\eta\eta}(f) &= co_{\eta\eta}(f) - iq_{\eta\eta}(f) \\ &= \int_0^{2\pi} p(f, \theta) \cos(kg \cos \theta + kh \sin \theta) d\theta \\ &\quad - i \int_0^{2\pi} p(f, \theta) \sin(kg \cos \theta + kh \sin \theta) d\theta \end{aligned} \quad (43)$$

Similarly, co- and quadrature- spectral density can be obtained for the wave properties as a function of f , in terms of $p(f, \theta)$.

Hereafter, () denotes $(kg \cos \theta + kh \sin \theta)$.

$$\left. \begin{aligned} co_{F_x F_x}(f) &= \int_0^{2\pi} (C_D''^2 + C_M''^2) p(f, \theta) \cos^2 \theta \cos() d\theta \\ q_{F_x F_x}(f) &= \int_0^{2\pi} (C_D''^2 + C_M''^2) p(f, \theta) \cos^2 \theta \sin() d\theta \end{aligned} \right\} \quad (44)$$

$$\left. \begin{aligned} co_{F_y F_y}(f) &= \int_0^{2\pi} (C_D''^2 + C_M''^2) p(f, \theta) \sin^2 \theta \cos() d\theta \\ q_{F_y F_y}(f) &= \int_0^{2\pi} (C_D''^2 + C_M''^2) p(f, \theta) \sin^2 \theta \sin() d\theta \end{aligned} \right\} \quad (45)$$

$$\left. \begin{aligned} co_{\eta F_x}(f) &= \int_0^{2\pi} C_D'' p(f, \theta) \cos \theta \cos() d\theta \\ &\quad + \int_0^{2\pi} C_M'' p(f, \theta) \cos \theta \sin() d\theta \end{aligned} \right\} \quad (46)$$

$$\left. \begin{aligned} q_{\eta F_x}(f) &= \int_0^{2\pi} C_D'' p(f, \theta) \cos \theta \sin() d\theta \\ &\quad + \int_0^{2\pi} C_M'' p(f, \theta) \cos \theta \cos() d\theta \end{aligned} \right\}$$

$$\left. \begin{aligned} co_{\eta F_y}(f) &= \int_0^{2\pi} C_D'' p(f, \theta) \sin \theta \cos() d\theta \\ &\quad + \int_0^{2\pi} C_M'' p(f, \theta) \sin \theta \sin() d\theta \end{aligned} \right\} \quad (47)$$

$$\left. \begin{aligned} q_{\eta F_y}(f) &= \int_0^{2\pi} C_D'' p(f, \theta) \sin \theta \sin() d\theta \\ &\quad + \int_0^{2\pi} C_M'' p(f, \theta) \sin \theta \cos() d\theta \end{aligned} \right\}$$

$$\left. \begin{aligned} \text{co}_{F_x F_y}(f) &= \int_0^{2\pi} (C_D''^2 + C_M''^2) p(f, \theta) \sin \theta \cos \theta \cos(\quad) d\theta \\ \text{q}_{F_x F_y}(f) &= \int_0^{2\pi} (C_D''^2 + C_M''^2) p(f, \theta) \sin \theta \cos \theta \sin(\quad) d\theta \end{aligned} \right\} \quad (48)$$

4.3 Directional spectrum for surface waves.

Since the co- and quadrature- spectrum in Eq. (43) through Eq. (48) can be obtained by the data, the problem becomes how to determine $p(f, \theta)$ in Eq. (43) through Eq. (48).

Let us assume that $p(f, \theta)$ can be formulated as

$$p(f, \theta) = P_\gamma(f) h(\theta) \quad (49)$$

$P_\gamma(f)$ is power spectrum for sea surface. According to Mobarek³⁾, $h(\theta)$ can be well represented by the probability density of the circular normal distribution^{17,18)} as follows:

$$h(\theta) = \frac{e^{a \cos(\theta-\gamma)}}{2\pi I_0(a)} \quad (50)$$

where a is a constant and a measure of the concentration around the mean, γ is a constant angle and at which the maximum energy is advancing, θ is the direction of advance for the wavelet, and $I_n(a)$ is the modified Bessel function of 1st kind. $\frac{1}{2\pi}$ is a normalizing factor which makes the integral, $\int_0^{2\pi} h(\theta) d\theta$, be unity. Because $I_n(a)$ is defined as

$$I_n(a) = \frac{1}{2\pi} \int_0^{2\pi} e^{a \cos \theta} \cos n\theta d\theta$$

when n is an integer, then

$$\frac{1}{2\pi I_0(a)} \int_0^{2\pi} e^{a \cos \theta} d\theta = 1$$

Some properties of the function given by Eq. (50) are that:

- (a) $h(\theta)$ is symmetric about $\theta = \gamma$
- (b) $h(\theta)$ has the maximum value, $\frac{e^a}{2\pi I_0(a)}$, at $\theta = \gamma$
- (c) $h(\theta)$ has approximate inflection point at $\theta = \gamma + \frac{1}{\sqrt{a}}$

Let $g = D \cos \beta$ and $h = D \sin \beta$, then,

$$kg \cos \theta + kh \sin \theta = kD \cos \beta \cos \theta + kD \sin \beta \sin \theta = kD \cos(\theta - \beta)$$

Eq. (43) becomes

$$\begin{aligned} P_{\gamma\gamma}(f) &= \int_0^{2\pi} p(f, \theta) [\cos\{kD \cos(\theta - \beta)\} - i \sin\{kD \cos(\theta - \beta)\}] d\theta \\ &= \int_0^{2\pi} p(f, \theta) e^{-ikD \cos(\theta - \beta)} d\theta \end{aligned}$$

Using Eq. (49) and Eq. (50),

$$P_{\eta\eta}(f) = \frac{P_{\eta}(f)}{2\pi I_0(a)} \int_0^{2\pi} e^{a \cos(\theta-\gamma)} e^{-ikD \cos(\theta-\beta)} d\theta.$$

Changing the variable so that

$$\theta - \gamma = \alpha \quad (55)$$

then, $\theta - \beta = \alpha + \gamma - \beta$ and

$$P_{\eta\eta}(f) = \frac{P_{\eta}(f)}{2\pi I_0(a)} \int_{-\gamma}^{2\pi-\gamma} e^{a \cos \alpha} e^{-ikD \cos(\alpha+\gamma-\beta)} d\alpha$$

Using the well known relation given by Eq. (56)

$$e^{a \cos \alpha} = I_0(a) + 2 \sum_{p=1}^{\infty} I_p(a) \cos(p\alpha) \quad (56)$$

the periodicity of the function, $e^{a \cos \alpha}$, and changing the order of integration and summation, then we obtain

$$\begin{aligned} P_{\eta\eta}(f) &= \frac{P_{\eta}(f) \times 2 \times I_0(a)}{2\pi I_0(a)} \int_0^{\pi} e^{-ikD \cos(\alpha+\gamma-\beta)} d\alpha \\ &+ \frac{P_{\eta}(f)}{\pi I_0(a)} \cdot 2 \sum_{p=1}^{\infty} I_p(a) \int_0^{\pi} \cos(p\alpha) e^{-ikD \cos(\alpha+\gamma-\beta)} d\alpha \end{aligned}$$

where p is an integer.

Changing the variable again so that

$$\alpha + \gamma - \beta = \lambda, \text{ then,}$$

$$\begin{aligned} P_{\eta\eta}(f) &= \frac{2I_0(a)P_{\eta}(f)}{2\pi I_0(a)} \int_0^{\pi} e^{-ikD \cos \lambda} d\lambda \\ &+ \frac{P_{\eta}(f)}{\pi I_0(a)} \times 2 \sum_{p=1}^{\infty} I_p(a) \int_0^{\pi} \cos\{p(\lambda-\gamma+\beta)\} e^{-ikD \cos \lambda} d\lambda \end{aligned}$$

Using the trigonometric identity

$$\cos\{p(\lambda-\gamma+\beta)\} = \cos(p\lambda) \cos\{p(\gamma-\beta)\} + \sin p\lambda \sin\{p(\gamma-\beta)\} \quad (57)$$

and paying attention to the fact that

$$\int_0^{\pi} e^{-ikD \cos \lambda} \cdot b \cdot \sin n\lambda d\lambda = 0 \quad (58)$$

then, the second term in the above equation becomes

$$\frac{P_{\eta}(f)}{\pi I_0(a)} \cdot 2 \sum_{p=1}^{\infty} I_p(a) \int_0^{\pi} \cos(p\lambda) \cos\{p(\gamma-\beta)\} e^{-ikD \cos \lambda} d\lambda$$

Using the expression for the Bessel function of 1st kind as follows:

$$J_n(x) = \frac{1}{\pi(-i)^n} \int_0^{\pi} e^{-ix \cos \alpha} \cos n\alpha d\alpha$$

$$= \frac{1}{\pi(i)^p} \int_0^\pi e^{iz \cos \alpha} \cos n \alpha d \alpha \quad (59)$$

The cross-spectral density between the time series $\eta(x, y, t)$ and $\eta(x+g, y+h, t)$ denoted as $P_{\eta\eta}(f)$, can be written

$$P_{\eta\eta}(f) = P_\eta(f) \left[J_0(kD) + \frac{2}{I_0(a)} \sum_{p=1}^{\infty} I_p(a) J_p(kD) \cos p(\gamma - \beta) (-i)^p \right] \quad (60)$$

After similar calculation for the wave property, the cross-spectrum density can be obtained in terms of the Bessel function and $p_\gamma(f)$ as follows:

Let $P_{F_x F_x}(f)$ be the cross-spectral density between the time series $F_x(x, y, t)$ and $F_x(x+g, y+h, t)$ then

$$\begin{aligned} P_{F_x F_x}(f) = & \frac{p_\gamma(f)(C_D'^{1/2} + C_M'^{1/2})}{2} \left[J_0(kD) + \cos 2\beta J_2(kD) (-i)^2 \right. \\ & + \sum_{p=1}^{\infty} \left\{ \frac{2 \cdot I_p(a)}{I_0(a)} J_p(kD) \cos p(\gamma - \beta) (-i)^p \right. \\ & + \frac{I_p(a)}{I_0(a)} \cos \{p\gamma + (2-p)\beta\} (-i)^{p-2} J_{p-2}(kD) \\ & \left. \left. + \frac{I_p(a)}{I_0(a)} \cos \{p\gamma - (2+p)\beta\} (-i)^{p+2} J_{p+2}(kD) \right\} \right] \quad (61) \end{aligned}$$

$$\begin{aligned} P_{F_y F_y}(f) = & \frac{P_\eta(f)(C_D'^{1/2} + C_M'^{1/2})}{2} \left[J_0(kD) - \cos 2\beta J_2(kD) (-i)^2 \right. \\ & + \sum_{p=1}^{\infty} \left\{ \frac{2 \times I_p(a)}{I_0(a)} J_p(kD) \cos p(\gamma - \beta) (-i)^p \right. \\ & - \frac{I_p(a)}{I_0(a)} \cos \{p\gamma + (2-p)\beta\} (-i)^{p-2} J_{p-2}(kD) \\ & \left. \left. - \frac{I_p(a)}{I_0(a)} \cos \{p\gamma - (2+p)\beta\} (-i)^{p+2} J_{p+2}(kD) \right\} \right] \quad (62) \end{aligned}$$

$$\begin{aligned} P_{F_x F_y}(f) = & \frac{P_\eta(f)(C_D'^{1/2} + C_M'^{1/2})}{2} \left[\sin 2\beta J_2(kD) (-i)^2 \right. \\ & + \sum_{p=1}^{\infty} \frac{I_p(a)}{I_0(a)} \sin \{(2+p)\beta - p\gamma\} J_{p+2}(kD) (-i)^{p+2} \\ & \left. + \sum_{p=1}^{\infty} \frac{I_p(a)}{I_0(a)} \sin \{(2-p)\beta + p\gamma\} J_{p-2}(kD) (-i)^{p-2} \right] \quad (63) \end{aligned}$$

$$\begin{aligned} P_{\eta F_x}(f) = & C_B'' \cdot \text{Real}\{L(a, \gamma)\} + C_M'' \cdot \text{Imag}\{L(a, \gamma)\} \\ & - i C_B'' \times \text{Imag}\{L(a, \gamma)\} - i C_M'' \text{Real}\{L(a, \gamma)\} \end{aligned}$$

where

$$L(a, \gamma) = P_\eta(f) \left[i \cos \beta \cdot J_1(kD) + \sum_{p=1}^{\infty} \frac{I_p(a)}{I_0(a)} \cos \{p\gamma + (1-p)\beta\} i^{p-1} J_{p-1}(kD) \right]$$

Determination of Approximate Directional Spectra for Coastal Waves

$$+ \sum_{p=1}^{\infty} \frac{I_p(a)}{I_0(a)} \cos \{p\gamma - (1+p)\beta\} i^{p+1} J_{p+1}(kD) \Big] \quad (64)$$

$$P_{\gamma, F_y}(f) = C''_D \cdot \text{Real} \{L'(a, \gamma)\} + C''_M \cdot \text{Imag} \{L'(a, \gamma)\} \\ - iC''_D \text{Imag} \{L'(a, \gamma)\} - iC''_M \text{Real} \{L'(a, \gamma)\}$$

where

$$L'(a, \gamma) = P_{\gamma}(f) \left[i \sin \beta \cdot J_1(kD) + \sum_{p=1}^{\infty} \frac{I_p(a)}{I_0(a)} \sin \{p\gamma + (1-p)\beta\} (i)^{p-1} J_{p-1}(kD) \right. \\ \left. - \sum_{p=1}^{\infty} \frac{I_p(a)}{I_0(a)} \sin \{p\gamma - (1+p)\beta\} (i)^{p+1} J_{p+1}(kD) \right] \quad (65)$$

The unknown parameters, a and γ , in Eq. (50) can be determined by means of the least square fitting method using the Eq. (60) through (65). For the actual computation, co- and quadrature- spectrum should be written separately and the values, a and γ , should be calculated for each co- and quadrature- spectrum.

4.4 Simplification of the Representations for the Wave Properties

The geographical condition of the wave meter and the wave direction meter

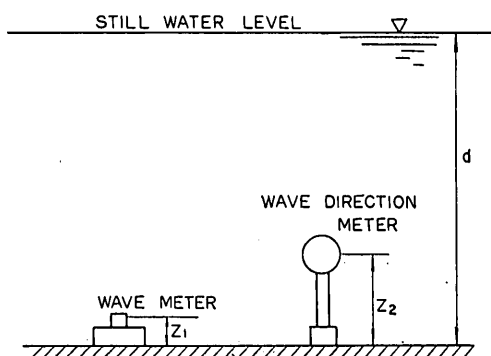


Fig. 1. Schematic figure of the installation of the wave meter and the wave direction meter

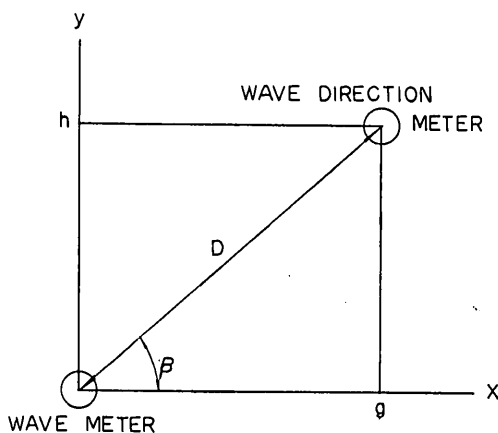


Fig. 2. Relationship between the wave meter installation point and the wave direction meter installation point

may be as shown in Fig. 1 and Fig. 2. The horizontal distance, D , between the wave meter and the wave direction meter could be small enough to be neglected in comparison with the wave length, that is

$$D \doteq 0 \quad (66)$$

then, g and h may be approximately zero. Therefore, the term, $(kg \cos \theta + kh \sin \theta)$, in Eqs. (43) through (48) may be approximately zero, that is

$$kg \cos \theta + kh \sin \theta \doteq 0 \quad (67)$$

In substituting Eq. (67) into Eqs. (43) through (48), following results are obtained.

$$\hat{P}_{\gamma\gamma}(f) = \hat{c}o_{\gamma\gamma}(f) = \int_0^{2\pi} p(f, \theta) d\theta = P_{\gamma}(f) \quad (68)$$

$$\hat{P}_{F_x F_x}(f) = \hat{c}o_{F_x F_x}(f) = \{(C_D'')^2 + (C_M'')^2\} \int_0^{2\pi} p(f, \theta) \cos^2 \theta d\theta = P_{F_x}(f) \quad (69)$$

$$\hat{P}_{F_y F_y}(f) = \hat{c}o_{F_y F_y}(f) = \{(C_D'')^2 + (C_M'')^2\} \int_0^{2\pi} p(f, \theta) \sin^2 \theta d\theta = P_{F_y}(f) \quad (70)$$

where $P_{F_x}(f)$ and $P_{F_y}(f)$ denote power spectra for F_x and F_y respectively.

$$\begin{aligned} \hat{P}_{\gamma F_x}(f) &= c o_{\gamma F_x}(f) - i \hat{q}_{\gamma F_x}(f) \\ &= C_D'' \int_0^{2\pi} p(f, \theta) \cos \theta d\theta - i C_M'' \int_0^{2\pi} p(f, \theta) \cos \theta d\theta \end{aligned} \quad (71)$$

$$\begin{aligned} \hat{P}_{\gamma F_y}(f) &= \hat{c}o_{\gamma F_y}(f) - i \hat{q}_{\gamma F_y}(f) \\ &= C_D'' \int_0^{2\pi} p(f, \theta) \sin \theta d\theta - i C_M'' \int_0^{2\pi} p(f, \theta) \sin \theta d\theta \end{aligned} \quad (72)$$

$$\hat{P}_{F_x F_y}(f) = \hat{c}o_{F_x F_y}(f) = \{(C_D'')^2 + (C_M'')^2\} \int_0^{2\pi} p(f, \theta) \sin \theta \cos \theta d\theta \quad (73)$$

These relationships can be obtained by Eqs. (28), (31) through (36), assuming g and $h=0$.

Eqs. (69) through (73) are written in terms of the modified Bessel function of 1st kind assuming that $p(f, \theta)$ can be formulated by Eq. (49) and Eq. (50) as before.

$$\hat{P}_{F_x F_x}(f) = \{(C_D'')^2 + (C_M'')^2\} \frac{P_{\gamma}(f)}{2} \left\{ 1 + \cos 2\gamma \frac{I_2(a)}{I_0(a)} \right\} \quad (74)$$

$$\hat{P}_{F_y F_y}(f) = \{(C_D'')^2 + (C_M'')^2\} \frac{P_{\gamma}(f)}{2} \left\{ 1 - \cos 2\gamma \frac{I_2(a)}{I_0(a)} \right\} \quad (75)$$

$$\begin{aligned} \hat{P}_{\gamma F_x}(f) &= \hat{c}o_{\gamma F_x}(f) - i \hat{q}_{\gamma F_x}(f) \\ &= C_D'' P_{\gamma}(f) \cos \gamma \frac{I_1(a)}{I_0(a)} - i C_M'' P_{\gamma}(f) \cos \gamma \frac{I_1(a)}{I_0(a)} \end{aligned} \quad (76)$$

$$\begin{aligned}\hat{P}_{\gamma F_y}(f) &= \hat{c}\partial_{\gamma F_y}(f) - i\hat{q}_{\gamma F_x}(f) \\ &= C''_D P_\gamma(f) \sin \gamma \frac{I_1(a)}{I_0(a)} - iC''_M P_\gamma(f) \sin \gamma \frac{I_1(a)}{I_0(a)}\end{aligned}\quad (77)$$

$$\hat{P}_{F_x F_y}(f) = \{(C''_D)^2 + (C''_M)^2\} \frac{P_\gamma(f)}{2} \sin 2\gamma \frac{I_2(a)}{I_0(a)} \quad (78)$$

Since Eq. (76) and Eq. (77) consist of co- and quadrature- spectrum while the others such as Eq. (74), (75), and (78) contain only co-spectrum, seven relations are available to determine the values, a and γ , in Eq. (50). Therefore the values can be determined by $7C_2=21$ pairs of the relations in the sense of the least square method. Plotting the obtained a and γ values in (a, γ) plane, the most probable value for a and γ can be obtained. Since the relations given by Eq. (75) through Eq. (78) would hold for each frequency, f , then a and γ might be a function of frequency.

The values, a and γ , also can be determined by the only one time use of whole relations given by Eq. (68), and Eq. (74) through Eq. (78).

Subtracting Eq. (74) from Eq. (75), we obtain

$$\hat{c}\partial_{F_x F_x}(f) - \hat{c}\partial_{F_y F_y}(f) = \{(C''_D)^2 + (C''_M)^2\} P_\gamma(f) \cos 2\gamma \frac{I_2(a)}{I_0(a)} \quad (79)$$

By Eq. (78), Eq. (79) and well known trigonometric identity such as

$$\cos^2 2\gamma + \sin^2 2\gamma = 1$$

$\frac{I_0(a)}{I_2(a)}$ can be obtained in terms of the results of the calculation of the data.

$$\frac{I_0(a)}{I_2(a)} = \frac{\{(C''_D)^2 + (C''_M)^2\} P_\gamma(f)}{\sqrt{\{\hat{c}\partial_{F_x F_x}(f) - \hat{c}\partial_{F_y F_y}(f)\}^2 + \{2 \cdot \hat{c}\partial_{F_x F_y}(f)\}^2}} \quad (80)$$

Substituting Eq. (80) into Eq. (78) and Eq. (79), $\cos 2\gamma$ and $\sin 2\gamma$ can be obtained as

$$\cos 2\gamma = \frac{\hat{c}\partial_{F_x F_x}(f) - \hat{c}\partial_{F_y F_y}(f)}{\sqrt{\{\hat{c}\partial_{F_x F_x}(f) - \hat{c}\partial_{F_y F_y}(f)\}^2 + \{2 \cdot \hat{c}\partial_{F_x F_y}(f)\}^2}} \quad (81)$$

$$\sin 2\gamma = \frac{2 \cdot \hat{c}\partial_{F_x F_y}(f)}{\sqrt{\{\hat{c}\partial_{F_x F_x}(f) - \hat{c}\partial_{F_y F_y}(f)\}^2 + \{2 \cdot \hat{c}\partial_{F_x F_y}(f)\}^2}} \quad (82)$$

Similarly, by Eq. (77) and Eq. (76), $\frac{I_0(a)}{I_1(a)}$, $\cos \gamma$, and $\sin \gamma$ values can be obtained as follows:

$$\frac{I_0(a)}{I_1(a)} = \frac{C''_D P_\gamma(f)}{\sqrt{\{\hat{c}\partial_{\gamma F_x}(f)\}^2 + \{\hat{c}\partial_{\gamma F_y}(f)\}^2}} = \frac{C''_M P_\gamma(f)}{\sqrt{\{\hat{q}_{\gamma F_x}(f)\}^2 + \{\hat{q}_{\gamma F_y}(f)\}^2}} \quad (83)$$

$$\cos \gamma = \frac{\hat{c}\partial_{\gamma F_x}(f)}{\sqrt{\{\hat{c}\partial_{\gamma F_x}(f)\}^2 + \{\hat{c}\partial_{\gamma F_y}(f)\}^2}} = \frac{\hat{q}_{\gamma F_x}(f)}{\sqrt{\{\hat{q}_{\gamma F_x}(f)\}^2 + \{\hat{q}_{\gamma F_y}(f)\}^2}} \quad (84)$$

$$\sin \gamma = \frac{\hat{c}\partial_{\gamma F_y}(f)}{\sqrt{\{\hat{c}\partial_{\gamma F_x}(f)\}^2 + \{\hat{c}\partial_{\gamma F_y}(f)\}^2}} = \frac{\hat{q}_{\gamma F_y}(f)}{\sqrt{\{\hat{q}_{\gamma F_x}(f)\}^2 + \{\hat{q}_{\gamma F_y}(f)\}^2}} \quad (85)$$

Taking the average value of a and γ , which are estimated by Eqs. (80) through (85), an approximate pair of a and γ can be obtained for each frequency. It is very interesting to note that the expressions for sine and cosine values do not include the unknown factors C_D and C_M .

4.5 Application for the Use of a Pressure-type Wave Meter

Since the pressure fluctuation η_p , at the pressure gauge, caused by the surface wave can be given by Eq. (14), the cross- and auto-spectral density for the fluctuation and the x, y component of the wave force in terms of power spectral density of the pressure fluctuation, $P_{\eta_p}(f)$, can be written as follows in the simplified method.

$$P_{\eta_p}(f) = w^2 \left(\frac{\cosh kz_1}{\cosh kd} \right)^2 P_\gamma(f) \quad (86)$$

$$\hat{P}_{F_x F_x}(f) = \{(C_D''')^2 + (C_M''')^2\} \frac{\hat{P}_{\eta_p}(f)}{2} \left\{ 1 + \cos 2\gamma \frac{I_2(a)}{I_0(a)} \right\} \quad (87)$$

$$\hat{P}_{F_y F_y}(f) = \{(C_D''')^2 + (C_M''')^2\} \frac{\hat{P}_{\eta_p}(f)}{2} \left\{ 1 - \cos 2\gamma \frac{I_2(a)}{I_0(a)} \right\} \quad (88)$$

$$\begin{aligned} \hat{P}_{\eta_p F_x}(f) &= \hat{c} \hat{\sigma}_{\eta_p F_x}(f) - i \hat{q}_{\eta_p F_x}(f) \\ &= \{C_D''' - iC_M'''\} \hat{P}_{\eta_p}(f) \cos \gamma \frac{I_1(a)}{I_0(a)} \end{aligned} \quad (89)$$

$$\begin{aligned} \hat{P}_{\eta_p F_y}(f) &= \hat{c} \hat{\sigma}_{\eta_p F_y}(f) - i \hat{q}_{\eta_p F_y}(f) \\ &= \{C_D''' - iC_M'''\} \hat{P}_{\eta_p}(f) \sin \gamma \frac{I_1(a)}{I_0(a)} \end{aligned} \quad (90)$$

$$\hat{P}_{F_x F_y}(f) = \{(C_D''')^2 + (C_M''')^2\} \frac{\hat{P}_{\eta_p}(f)}{2} \sin 2\gamma \frac{I_2(a)}{I_0(a)} \quad (91)$$

where C_D''' and C_M''' are redefined as

$$\begin{aligned} C_D''' &= C_D'' \times \left(\frac{\cosh kd}{\cosh kz_1} \right) \cdot \frac{1}{w} \\ &= \frac{C_D}{2g} (\pi r^2) \cdot V_{rms} \sqrt{\frac{8}{\pi}} \cdot \left(\frac{\cosh kd}{\cosh kz_1} \right) \left(\frac{\cosh kz_2}{\sinh kd} \right) (2\pi f) \end{aligned} \quad (92)$$

$$\begin{aligned} C_M''' &= C_M'' \times \left(\frac{\cosh kd}{\cosh kz_1} \right) \cdot \frac{1}{w} \\ &= \frac{C_M}{g} \left(\frac{4}{3} \pi r^3 \right) \left(\frac{\cosh kd}{\cosh kz_1} \right) \left(\frac{\cosh kz_2}{\sinh kd} \right) (2\pi f)^3 \end{aligned} \quad (93)$$

where z_1 is the installation depth of the wave meter measured along the z axis (from the bottom of the sea) and z_2 is the position of the center of the sphere (from the bottom, See Fig. 1).

The constant, V_{rms} , can be calculated by the following equation.

$$V_{rms} = \sqrt{2 \int_0^{\infty} P_v(f) df} \quad (94)$$

where $P_v(f)$ is power spectral density for the velocity and can be written as¹⁰⁾

$$P_v(f) = (2\pi f)^2 \left(\frac{\cosh kz_2}{\sinh kd} \right)^2 P_\eta(f) \quad (95)$$

Combining Eq. (86) with Eq. (95) and substituting it into Eq. (94), V_{rms} value can be obtained in terms of the power spectral density for the pressure fluctuation, $P_{\eta_p}(f)$, as follows:

$$V_{rms} = \sqrt{2 \int_0^{\infty} (2\pi f)^2 \left(\frac{\cosh kz_2}{\sinh kd} \right)^2 \frac{1}{\omega^2} \left(\frac{\cosh kd}{\cosh kz_1} \right)^2 P_{\eta_p}(f) df} \quad (96)$$

For the engineering problems, C_D and C_M can be assumed to be constants. These values, however, might be a function of frequency. By the relationships given by Eq. (86) through Eq. (91), C_D''' and C_M''' are obtained as

$$C_{DX}''' = \sqrt{\frac{(\hat{P}_{F_x F_x}(f) + \hat{P}_{F_y F_y}(f)) \times (\hat{c}\partial_{\eta_p F_x}(f))^2}{\hat{P}_{\eta_p}(f) \{ (\hat{c}\partial_{\eta_p F_x}(f))^2 + (\hat{q}_{\eta_p F_x}(f))^2 \}}} \quad (97)$$

$$C_{DY}''' = \sqrt{\frac{(\hat{P}_{F_x F_x}(f) + \hat{P}_{F_y F_y}(f)) \times (\hat{c}\partial_{\eta_p F_y}(f))^2}{\hat{P}_{\eta_p}(f) \{ (\hat{c}\partial_{\eta_p F_y}(f))^2 + (\hat{q}_{\eta_p F_y}(f))^2 \}}} \quad (98)$$

$$C_{MX}''' = C_{DX}''' \cdot \sqrt{\frac{\{\hat{q}_{\eta_p F_x}(f)\}^2}{\{\hat{c}\partial_{\eta_p F_x}(f)\}^2}} \quad (99)$$

$$C_{MY}''' = C_{DY}''' \cdot \sqrt{\frac{\{\hat{q}_{\eta_p F_y}(f)\}^2}{\{\hat{c}\partial_{\eta_p F_y}(f)\}^2}} \quad (100)$$

Here, X means that the values are estimated by F_x , and Y by F_y .

Inserting Eq. (92) and Eq. (93) into Eqs. (97) through (100), C_D and C_M values are obtained as

$$C_D = \left(\frac{C_{DX}'''}{C_{DY}'''} \right) \cdot \left[\frac{1}{2g} (\pi r^2) \cdot V_{rms} \sqrt{\frac{8}{\pi}} \cdot \left(\frac{\cosh kd}{\cosh kz_1} \right) \left(\frac{\cosh kz_2}{\sinh kd} \right) (2\pi f) \right]^{-1} \quad (101)$$

$$C_M = \left(\frac{C_{MX}'''}{C_{MY}'''} \right) \cdot \left[\frac{4}{3g} \pi r^3 \left(\frac{\cosh kd}{\cosh kz_1} \right) \left(\frac{\cosh kz_2}{\sinh kd} \right) (2\pi f)^2 \right]^{-1} \quad (102)$$

a and γ values can be obtained by $\frac{I_0(a)}{I_2(a)}$, $\frac{I_0(a)}{I_1(a)}$, $\cos 2\gamma$, $\sin 2\gamma$, $\cos \gamma$, and $\sin \gamma$ in Eq. (80) through Eq. (85) replacing C_D' , C_M' , and η by C_D''' , C_M''' , and η_p , respectively. For example, $\frac{I_0(a)}{I_2(a)}$ and $\frac{I_0(a)}{I_1(a)}$ are to be obtained as follows.

$$\frac{I_0(a)}{I_2(a)} = \frac{\hat{P}_{F_x F_x}(f) + \hat{P}_{F_y F_y}(f)}{\sqrt{\{\hat{P}_{F_x F_x}(f) - \hat{P}_{F_y F_y}(f)\} + \{2 \cdot \hat{c}\partial_{F_x F_y}(f)\}^2}} \quad (103)$$

$$\frac{I_0(a)}{I_1(a)} = \left[\frac{P_{\eta_p}(f) \{P_{F_x F_x}(f) + P_{F_y F_y}(f)\} \cdot (\hat{c}\partial_{\eta_p F_x}(f))^2}{\{(\hat{c}\partial_{\eta_p F_x}(f))^2 + (\hat{q}_{\eta_p F_x}(f))^2\} \{(\hat{c}\partial_{\eta_p F_x}(f))^2 + (\hat{c}\partial_{\eta_p F_y}(f))^2\}} \right]^{1/2} \quad (104)$$

5. Investigation of the Accuracy of the Method by Means of Simulated Wave Properties

Three types of simulation are generally used; by hydraulic models, analogue models, and digital models. The former two have been used widely for many years. However, due to the space limit and financial difficulties, hydraulic models are often not feasible. More over, it can easily understood that to generate surface waves with directional spectra is almost impossible in the hydraulic model. An analogue model which is a mechanical or electric device that is designed to have properties equivalent to that of the system in consideration, sometimes, can not give the results with the desired accuracy.

On the other hand, digital models are relatively new approach. It is not only more accurate, but has also advantages of possessing convenient high speed.

Borgman¹⁶⁾ (1967) has suggested two possible ways such as linear digital filter and wave superposition, for carrying out a digital simulation process for wind waves. In this study, only the latter one was used.

5.1 Simulation for sea surfaces having a directional spectral density by wave superposition

Eq. (1), in the previous section, directly shows how to generate random sea surfaces by wave superposition. If the directional spectrum is known, sea surfaces, $\eta(x, y, t)$, can be obtained by carrying out the operation in Eq. (1). However, it is impossible to integrate the equation upto infinity in the frequency domain by discrete method. The maximum frequency should be determined for the completion of the integration. If a certain value is selected as the maximum frequency, f_{MAX} , and if an equally spaced subdivision, $f_n - f_{n-1}$, of the interval $(0, f_{\text{MAX}})$ is used, the obtained sea surface would have periodicity with the period of, $1/f$ where $f = \frac{f_{\text{MAX}}}{2M}$ and M is the number of the subdivided intervals.

In order to avoid the periodicity, one could select the set of f values with a random number table. Borgman¹⁶⁾ (1967), however, proposed another way based on the cumulative spectrum.

Let the directional spectrum be the form as given by Eq. (49) and $h(\theta)$ be the probability density of the circular normal distribution.

Then the cumulative spectrum, $S(f, \theta)$, for the directional spectrum is represented as

$$\begin{aligned} S(f, \theta) &= 2 \int_0^f \int_0^\theta h(\theta') p(f') d\theta' df' \\ &= 2 \int_0^f p(f') \left\{ \int_0^\theta h(\theta') d\theta' \right\} df' \end{aligned} \quad (105)$$

Therefore,

$$S(f, 2\pi) = 2 \int_0^f p(f') df' = \Pi(f) \quad (106)$$

Thus the corresponding value to $p(f_m) \Delta f_m$ in Eq. (1) nearly equals to $[\Pi(f_m) - \Pi(f_{m-1})]/2$.

Eq. (1) becomes

$$\eta'(x, y, t) = \sqrt{2} \sum_{m=1}^M \sum_{n=1}^N \sqrt{\Pi(f_m) - \Pi(f_{m-1})} \sqrt{h(\theta_n) \Delta\theta_n} \cdot \cos(k_m x \cos \theta_n + k_m y \sin \theta_n - 2\pi f_m t + \Phi_{mn}) \quad (107)$$

The periodicity due to f is avoided if the set of f_m values are chosen to make $\Pi(f_m) - \Pi(f_{m-1})$ constant, say equal to G^2 , for all m values. Then Eq. (107) becomes

$$\eta'(x, y, t) = \sqrt{2} \sum_{m=1}^M \sum_{n=1}^N G \sqrt{h(\theta_n) \Delta\theta_n} \cdot \cos(k_m x \cos \theta_n + k_m y \sin \theta - 2\pi f_m t + \Phi_{mn}) \quad (108)$$

with f_m defined as the solution of

$$\Pi(f_m) = \frac{m}{M} \Pi(\infty) \doteq \frac{m}{M} \Pi(f_{\text{MAX}}) \quad (109)$$

If the Bretschneider-Pierson spectral density is used as a theoretical model, Eq. (109) is easy to solve. The spectrum has the form

$$p_B(f) = \frac{AB}{f^6} e^{-B/f^4} \quad (110)$$

and the cumulative spectra is

$$\Pi(f) = 2 \int_0^f p_B(f') df' = \frac{A}{2} e^{-B/f^4} \quad (111)$$

Hence $\Pi(\infty) = A/2$ and the solution of Eq. (109) is

$$f_m = \left[\frac{B}{\log_e \left(\frac{M}{m} \right)} \right]^{1/4} \quad (112)$$

The energy density for the directional spectrum, $p(f, \theta)$, can be completely determined if the maximum frequency, f_{MAX} , power spectral peak frequency, f_p , total energy of the directional spectrum, $\Pi(\infty)$, a value and γ value are given.

The value B is determined from f_p if the derivative of $p_B(f)$ with respect to f is made equal to zero as

$$\frac{dp_B(f)}{df} = (-5 + 4Bf^{-4}) AB f^{-6} \cdot e^{-B/f^4} = 0 \quad (113)$$

$$B = \frac{5}{4} f_p^4 \quad (114)$$

The value A is determined as follows

$$\Pi(\infty) = 2 \int_0^\infty p_B(f) df \doteq 2 \int_0^{f_{\text{MAX}}} p_B(f) df = \frac{A}{2} e^{-B/f_{\text{MAX}}^4} \quad (115)$$

$$A \doteq 2\Pi(\infty) \cdot e^{B/f_{\text{MAX}}^4} \quad (116)$$

Equations for other wave properties are analogously obtained with the reference of Eqs. (106), (10), (11), (12), (13), (14), (21), and Eq. (22) as follows.

$$\begin{aligned}
 V'_x(x, y, z; t) &= \sqrt{2} \sum_{m=1}^M \sum_{n=1}^N G \sqrt{h(\theta_n) \Delta \theta_n} \cdot 2\pi f_m \\
 &\quad \times \cos \theta_n \frac{\cosh k_m z}{\sinh k_m d} \cos(k_m x \cos \theta_n + k_m y \sin \theta_n - 2\pi f_m t + \Phi_{mn})
 \end{aligned} \tag{117}$$

$$\begin{aligned}
 V'_y(x, y, z; t) &= \sqrt{2} \sum_{m=1}^M \sum_{n=1}^N G \sqrt{h(\theta_n) \Delta \theta_n} \cdot 2\pi f_m \\
 &\quad \times \sin \theta_n \frac{\cosh k_m z}{\sinh k_m d} \cos(k_m x \cos \theta_n + k_m y \sin \theta_n - 2\pi f_m t + \Phi_{mn})
 \end{aligned} \tag{118}$$

$$\begin{aligned}
 A'_x(x, y, z; t) &= \sqrt{2} \sum_{m=1}^M \sum_{n=1}^N G \sqrt{h(\theta_n) \Delta \theta_n} (2\pi f_m)^2 \\
 &\quad \times \cos \theta_n \left(\frac{\cosh k_m z}{\sinh k_m d} \right) \sin(k_m x \cos \theta_n + k_m y \sin \theta_n - 2\pi f_m t + \Phi_{mn})
 \end{aligned} \tag{119}$$

$$\begin{aligned}
 A'_y(x, y, z; t) &= \sqrt{2} \sum_{m=1}^M \sum_{n=1}^N G \sqrt{h(\theta_n) \Delta \theta_n} (2\pi f_m)^2 \\
 &\quad \times \sin \theta_n \left(\frac{\cosh k_m z}{\sinh k_m d} \right) \sin(k_m x \cos \theta_n + k_m y \sin \theta_n - 2\pi f_m t + \Phi_{mn})
 \end{aligned} \tag{120}$$

$$\begin{aligned}
 \eta'_p(x, y, z; t) &= \sqrt{2} \sum_{m=1}^M \sum_{n=1}^N G \sqrt{h(\theta_n) \Delta \theta_n} \cdot \left(\frac{\cosh k_m z}{\cosh k_m d} \right) \cdot \omega \\
 &\quad \times \cos(k_m x \cos \theta_n + k_m y \sin \theta_n - 2\pi f_m t + \Phi_{mn})
 \end{aligned} \tag{121}$$

G in Eq. (108), Eq. (117)~(121) is obtained as follows

$$G = \sqrt{H(f_m) - H(f_{m-1})} = \sqrt{\frac{H(\infty)}{M}} = \sqrt{\frac{\frac{A}{2} e^{-B/f^4_{\text{MAX}}}}{M}} \tag{122}$$

5.2 Method of generating random phases

The random phases, Φ_{mn} , in Eq. (108) could be obtained by means of a random number table. In this study, however, the pseudo-random phases have been generated by the multiplicative congruence method as follows.

Let the sequence of pseudo-random numbers be denoted by

$$\{X_n\}, \quad n=0, 1, 2, \dots$$

Then the multiplicative congruence method is

$$X_{n+1} = K \cdot X_n \pmod{M_0} \tag{123}$$

Determination of Approximate Directional Spectra for Coastal Waves

The choice of M_0 is determined by the capacity and base of the computer which is to be used; K is chosen so that: 1) the resulting sequence $\{X_n\}$ possesses the desired statistical properties of random numbers, 2) the period of the sequence is as long as possible, and 3) the speed of generation is fast.

In this case, M_0 and K were determined as 18731 and 399 respectively. The initial value, X_0 , was selected as 2581.

The random phases which distribute uniformly between $[0, 2\pi]$ are obtained as follows.

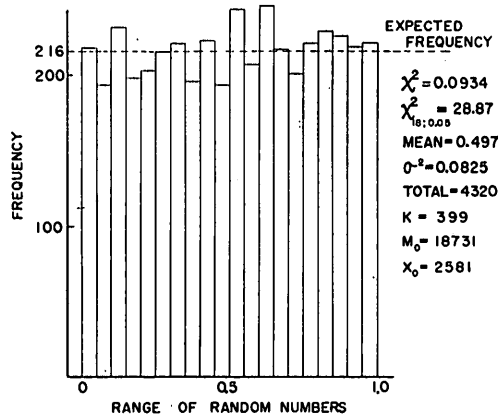


Fig. 3. Frequency histogram of the pseudo-random numbers used

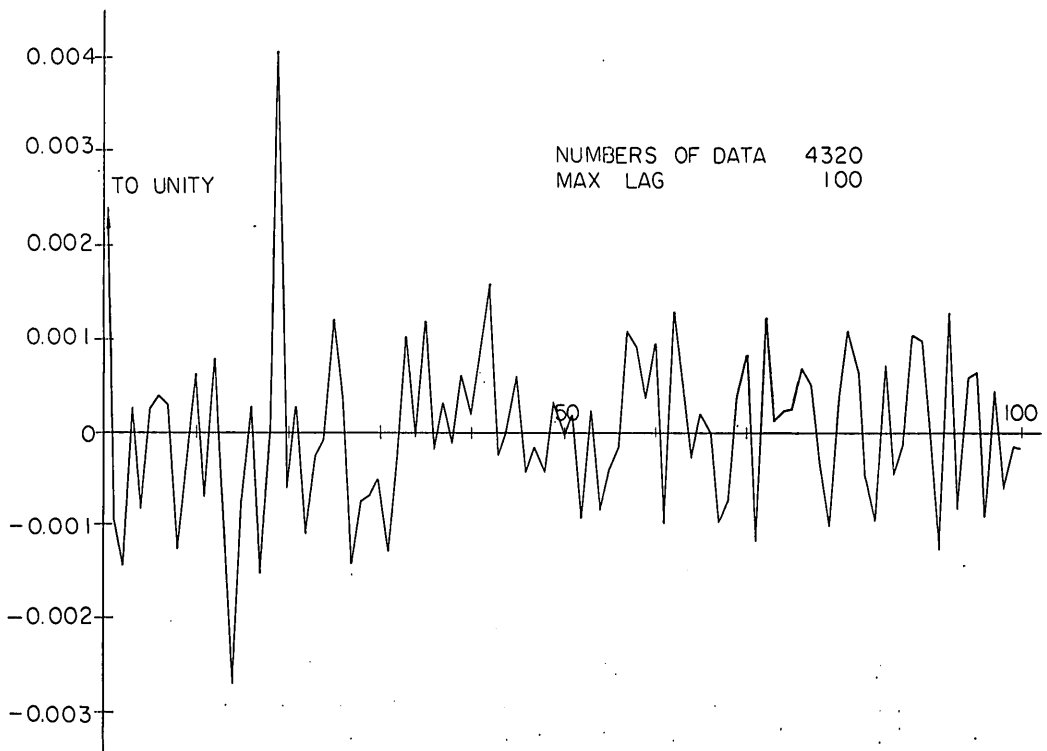


Fig. 4. Auto-correlogram for the pseudo-random numbers

$$\left. \begin{aligned} X_0 &= 2581 \\ X_n &= 399X_{n-1}(\text{Mod } 18731) \\ \Phi_n &= 2\pi \cdot X_n / 18731 \end{aligned} \right\} \quad (124)$$

Since the random phases Φ_n are the pseudo-random numbers, the quality of the random phase must be determined by several statistical tests. The results of the uniformness test for X_0 is shown in Fig. 3. Two kinds of the run tests based on runs above and below, and runs up and down proved the randomness of the random phases. Fig. 4 shows the auto-correlogram for the random phases. The largest correlation coefficient was 0.00409 up to the lag number of 100.

5.3 Generating the simulated wave properties

For the generation of the simulated wave properties, the directional spectra with one peak in frequency and in azimuth was used. The dimensions in Table 1. were used in order to generate the simulated wave properties.

Only two cases 1-d and 2-b were generated by the direct use of Eq. (108), and Eqs. (117)~(121). It is evident that the other cases in the same class can be obtained by multiplying the square root of the ratio of A . The simulated data for case 1-d and 2-b are shown in Table A-1 and A-2 in the appendix.

In these calculation, the (f, θ) plan was subdivided into 60 intervals in frequency and 72 in azimuth. Reduction of the range for the numerical integration was considered so that the computation time became fast. The range of the integration with respect to azimuth was decided to be $\pm 90^\circ$ centered γ instead of $\pm 180^\circ$. It is clear that the procedure is allowable if a value is large. The error due to the reduction was estimated as less than 0.01% of the maximum amplitude in the calculated series with the a value of 16.

After obtaining the simulated wave properties, it is easy to generate the simulated wave force acting on the sphere. The force was obtained by Eq. (19) and (20) as the linearized one and also by Eq. (125) and (126) as the non-linear one.

$$F_x = \frac{C_{D\omega}}{2g} \pi r^2 V_x |V| + \frac{C_{M\omega}}{g} \left(\frac{4\pi r^3}{3} \right) A_x \quad (125)$$

$$F_y = \frac{C_{D\omega}}{2g} \pi r^2 V_y |V| + \frac{C_{M\omega}}{g} \left(\frac{4\pi r^3}{3} \right) A_y \quad (126)$$

Table 1. Constants for the generation of simulated wave properties

| CASE | $f_p(\text{Hz})$ | $f_{\max}(\text{Hz})$ | A | B | a | γ | $I_0(a)$ | d | z_1 | z_2 | x | y |
|------|------------------|-----------------------|----------------|-----------------------|-----|----------|----------|-----|-------|-------|-----|-----|
| 1-a | 0.1 | 0.5 | ≈ 7200 | 1.25×10^{-4} | 16 | 60 | 893446.2 | 8.5 | 1.0 | 1.60 | 0 | 0 |
| 1-b | 0.1 | 0.5 | ≈ 4050 | 1.25×10^{-4} | 16 | 60 | 893446.2 | 8.5 | 1.0 | 1.60 | 0 | 0 |
| 1-c | 0.1 | 0.5 | ≈ 1800 | 1.25×10^{-4} | 16 | 60 | 893446.2 | 8.5 | 1.0 | 1.60 | 0 | 0 |
| 1-d | 0.1 | 0.5 | ≈ 450 | 1.25×10^{-4} | 16 | 60 | 893446.2 | 8.5 | 1.0 | 1.60 | 0 | 0 |
| 2-a | 0.1 | 0.5 | ≈ 7200 | 1.25×10^{-4} | 15 | 40 | 339649.4 | 8.5 | 1.0 | 1.60 | 0 | 0 |
| 2-b | 0.1 | 0.5 | ≈ 4050 | 1.25×10^{-4} | 15 | 40 | 339649.4 | 8.5 | 1.0 | 1.60 | 0 | 0 |
| 2-c | 0.1 | 0.5 | ≈ 1800 | 1.25×10^{-4} | 15 | 40 | 339649.4 | 8.5 | 1.0 | 1.60 | 0 | 0 |
| 2-d | 0.1 | 0.5 | ≈ 450 | 1.25×10^{-4} | 15 | 40 | 339649.4 | 8.5 | 1.0 | 1.60 | 0 | 0 |

where $|V|$ is equal to $\sqrt{V_x^2 + V_y^2}$.

In calculating the simulated force, the radius of the sphere, r , was set to be 6 cm and C_D and C_M values were considered as constants for each case. The root-mean-square value of horizontal component of water particle velocity in unidirectional case must be obtained when the force by Eq. (19) and (20) are used. The following two equations are available for the estimation of the root-mean-square value as well as Eq. (96).

$$V_{rms} = \sqrt{2 \int_0^\infty (2\pi f)^2 \left(\frac{\cosh kmz_1}{\sinh kmd} \right)^2 P_\gamma(f) df} \quad (127)$$

$$V_{rms} = \sqrt{\frac{1}{N} \sum_{i=1}^N (V_{x_i}^2 + V_{y_i}^2)} \quad (128)$$

The difference among the three was small. Then Eq. (96) was used for the calculation.

5.4 Accuracy of the method

Each wave property was generated at a period of one second for 600 seconds. In this section, the directional spectrum which are obtained by means of the simulation data will be compared with the given directional spectrum. For the wave force, both pair of Eq. (19), (20) and of Eq. (125), (126) were used and their results will be discussed. Since the directional spectrum is determined a and γ value in the method, the discussion will mainly be done on the two values. For the calculation of a and γ value and other values, η_p , F_x , and F_y were used.

Fig. 5 and Fig. 6 show the change of a value with respect to the frequency

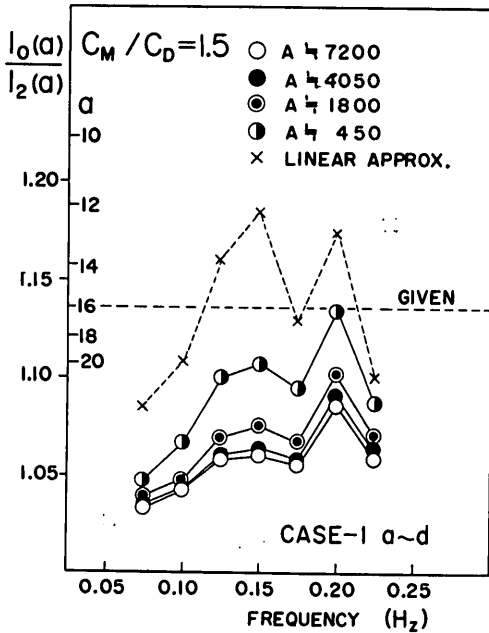


Fig. 5. Change of $\frac{I_0(a)}{I_2(a)}$ value due to A in case 1

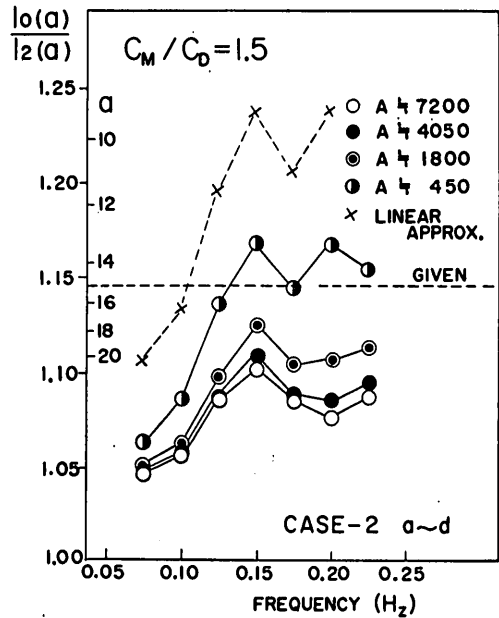


Fig. 6. Change of $\frac{I_0(a)}{I_2(a)}$ value due to A in case 2

and A value. Resulting a value from the force by linearized drag term denoted, \times , deviates from the given value. The deviation may correspond to the errors due to the spectral analysis, the method of simulation, and the many assumptions made. Because there might be no difference between the values provided that there had not been any errors in the calculations. The change of the a value by means of the linearized force was not large enough to plot separately with respect to A value. This can be also said of other values which will be discussed here. The difference between the value resulting from the use of linearized drag term for force component and the values which were obtained by means of the force calculated by the non-linear drag term, would be caused by the linear approximation for the drag term in the force formula. The difference decreases when A value decreases. However, the a value obtained by the use of the non-linear drag term is larger than the given a value by two or more times. This means that the a value obtained by the method is larger than the actual value.

Fig. 7 and Fig. 8 show the behaviour of the a value obtained from Eq. (83). The behaviour seems to be the same as the a value in Fig. 5 and Fig. 6. But the $\frac{I_0(a)}{I_1(a)}$ values in Fig. 7 and Fig. 8, sometimes, fall down below 1.00. Since $I_0(a)$ is always larger than $I_1(a)$, a value obtained by $\frac{I_0(a)}{I_3(a)}$ value should be used for the estimation of the value.

Fig. 9 and Fig. 10 show the change of γ value with respect to A value and frequency. It was obtained by the results from Eq. (82). It could be said that there was little difference between the plotted points for fixed frequency. This means that the γ value is not affected much by the linear-approximation. However, the deviation from the given value changes remarkably when γ value changes.

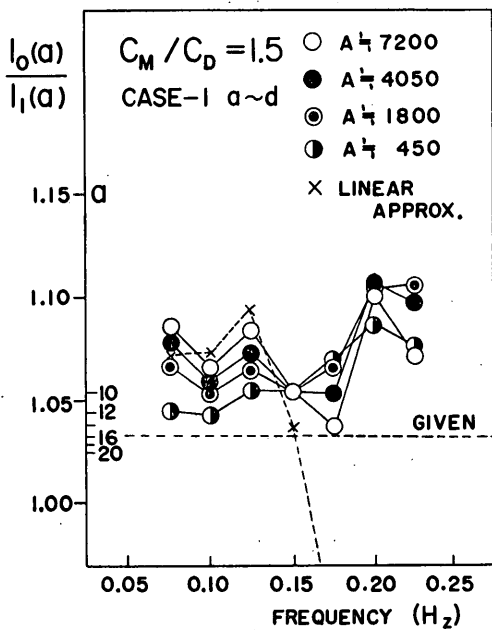


Fig. 7. Change of $\frac{I_0(a)}{I_1(a)}$ value due to A in case 1

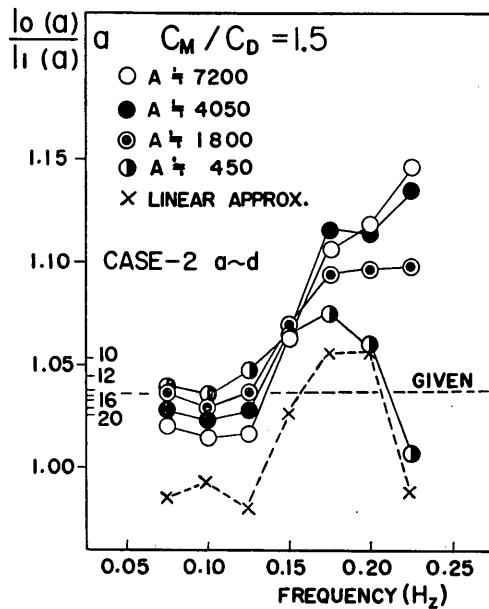


Fig. 8. Change of $\frac{I_0(a)}{I_1(a)}$ value due to A in case 2

Determination of Approximate Directional Spectra for Coastal Waves

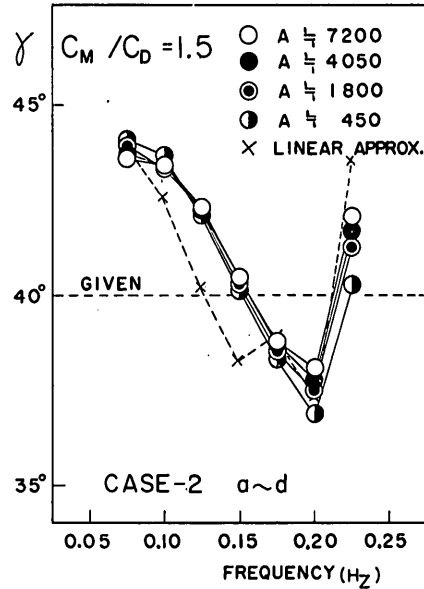
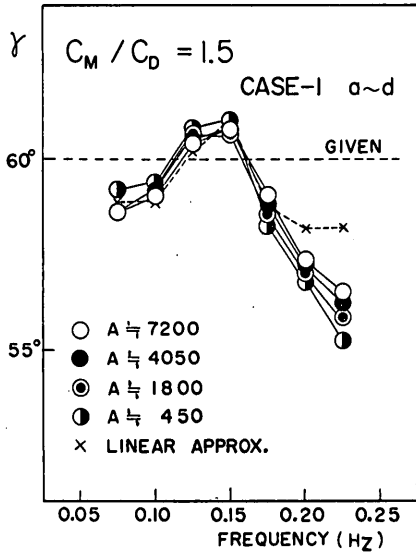


Fig. 9. Change of γ value due to A in case 1 Fig. 10. Change of γ value due to A in case 2

Looking at Fig. 11~14 where the obtained C_D and C_M values are shown, the same features as γ value may be recognized, that is, the value C_D and C_M are not affected either by the change of A value or by the linear-approximation.

Let the value A be fixed and C_M/C_D value be changed.

Fig. 15 and Fig. 16 show the change of a and γ value for fixed A with respect to C_M/C_D value and frequency. The value γ is not affected by the change

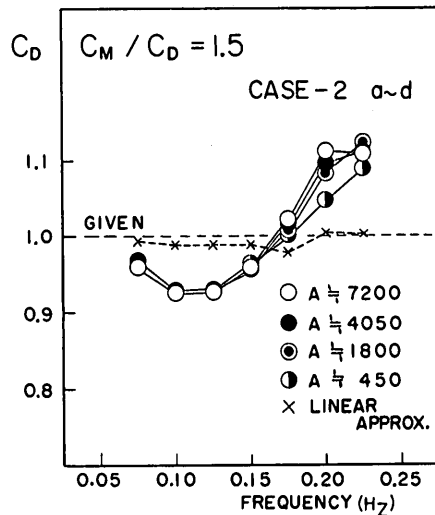
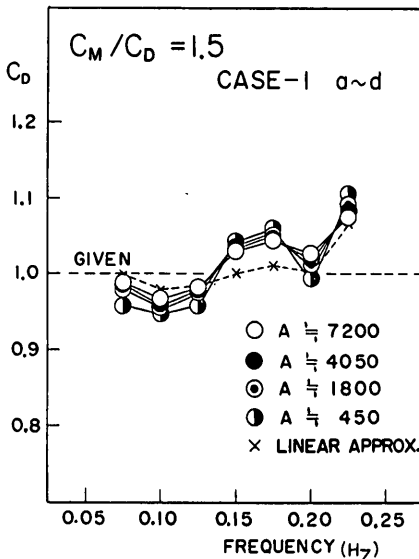


Fig. 11. Change of C_D value due to A in case 1

Fig. 12. Change of C_D value due to A in case 2

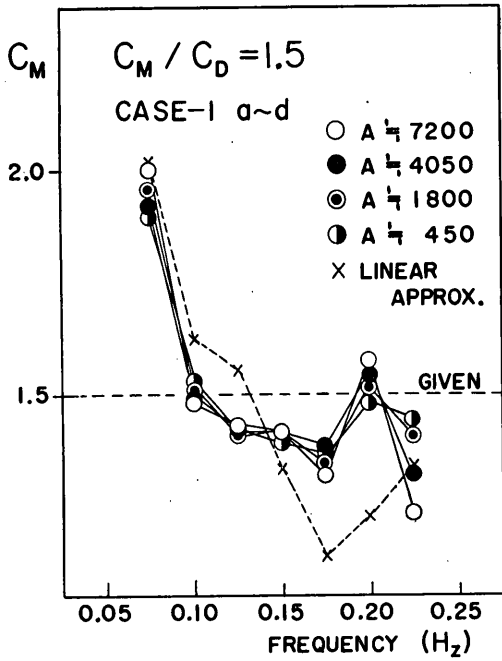


Fig. 13. Change of C_M value due to A in case 1

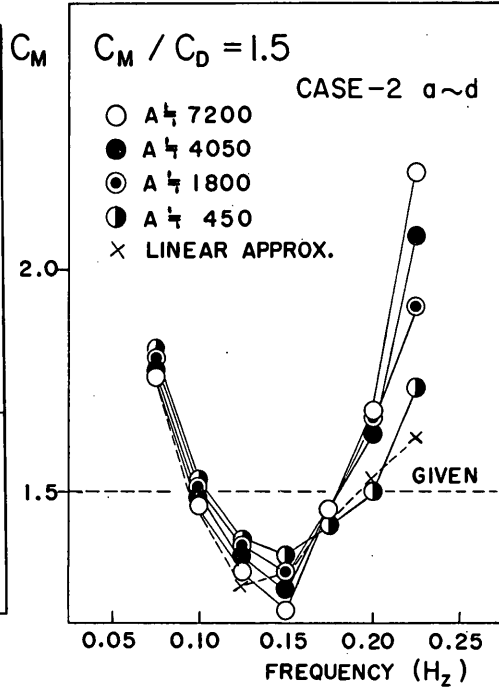


Fig. 14. Change of C_M value due to A in case 2

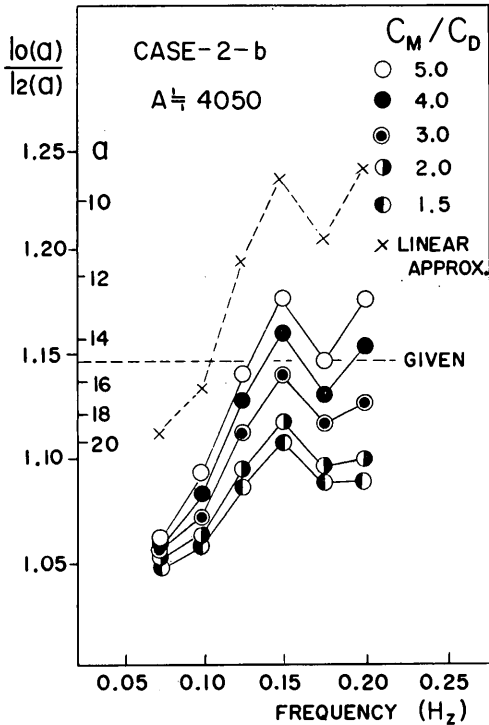


Fig. 15. Change of $I_0(a)/I_2(a)$ value due to C_M/C_D

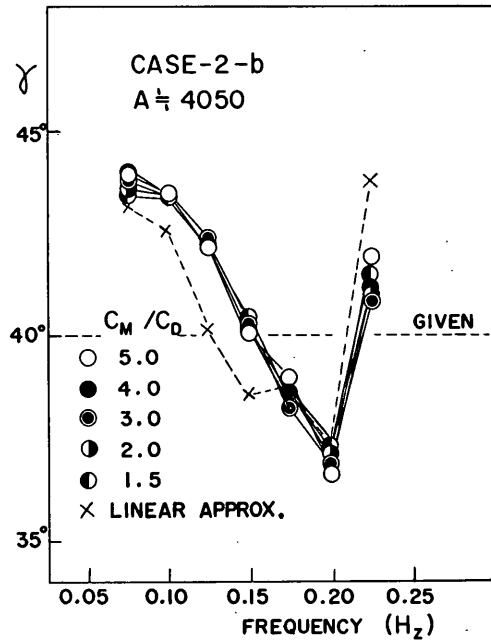


Fig. 16. Change of γ value due to C_M/C_D

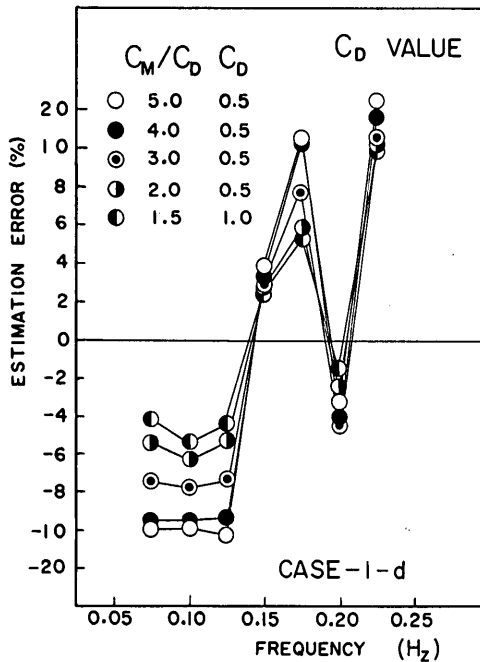


Fig. 17. Effect of the C_M/C_D on the estimation error of C_D

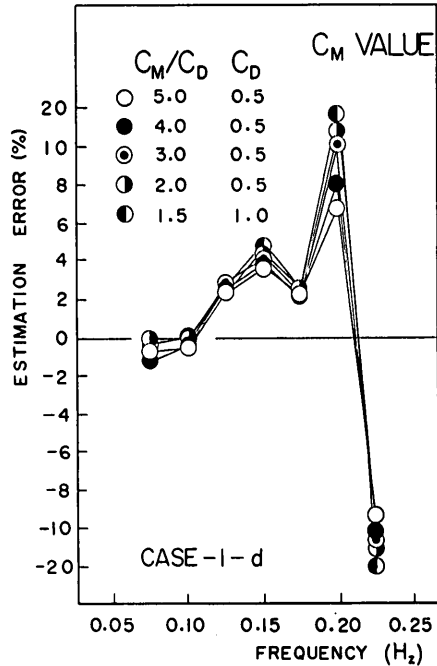


Fig. 18. Effect of the C_M/C_D on the estimation error of C_M

of C_M/C_D . Comparing Fig. 16 with Fig. 10, the obtained γ value for each frequency is almost the same for each other. The value a in Fig. 16 remarkably changes with respect to C_M/C_D . It becomes close to the a value from the linearized force, when C_M/C_D value increases. This is reasonable, because C_D is the constant of the linearized drag term.

How does the estimation error of C_D and C_M change when C_M/C_D value changes? Fig. 17 and 18 show the relative error to the given value.

In summary, the linear-approximation has little effect on the estimation of γ , C_D , and C_M for the given directional spectrum at the given geographical situation. The value a , however, is affected by the magnitude of the total energy of the given wave system and the ratio of C_M and C_D value.

The directional spectrum can be easily figured out by using Eq. (49). For $C_D=0.5$, $C_M=1.5$, $A \approx 450$, $a=16$, and $\gamma=60^\circ$, the given directional spectrum is shown as Fig. 19, the directional spectrum by the method using the linearized force formula, as Fig. 20, and the directional spectrum by the method using the non-linear drag term for force equation, as Fig. 21. Comparing Fig. 20 with Fig. 21, it is found that there is no significant difference between them.

The method of the spectral analysis followed the method by Bendat and Piersol¹⁹⁾ (1966) with the Hamming spectral window of 0.23, 0.54, and 0.23. In order to get higher degree of freedom in spectral analysis, the maximum lag time was chosen as 20 second. This results in the degree of freedom being about 60. In finding the a value from the ratio of the modified Bessel functions, $I_0(a)/I_1(a)$ and $I_0(a)/I_2(a)$, the Handbook of Mathematical Function with Formulas, Graphs, and Mathematical Tables²⁰⁾ was used. For large value of a , following polynomial approximations were used.

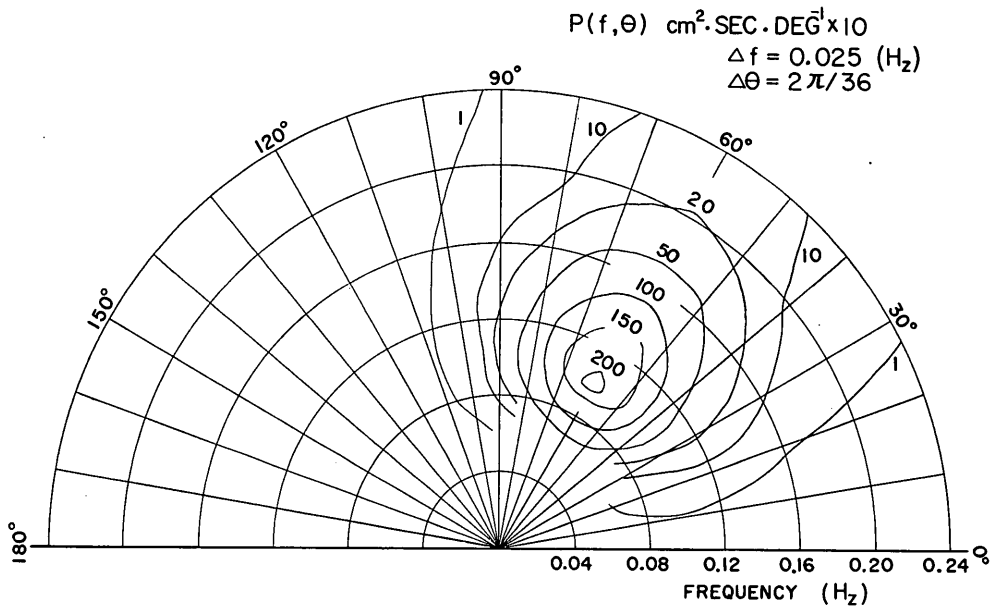


Fig. 19. Given directional spectrum

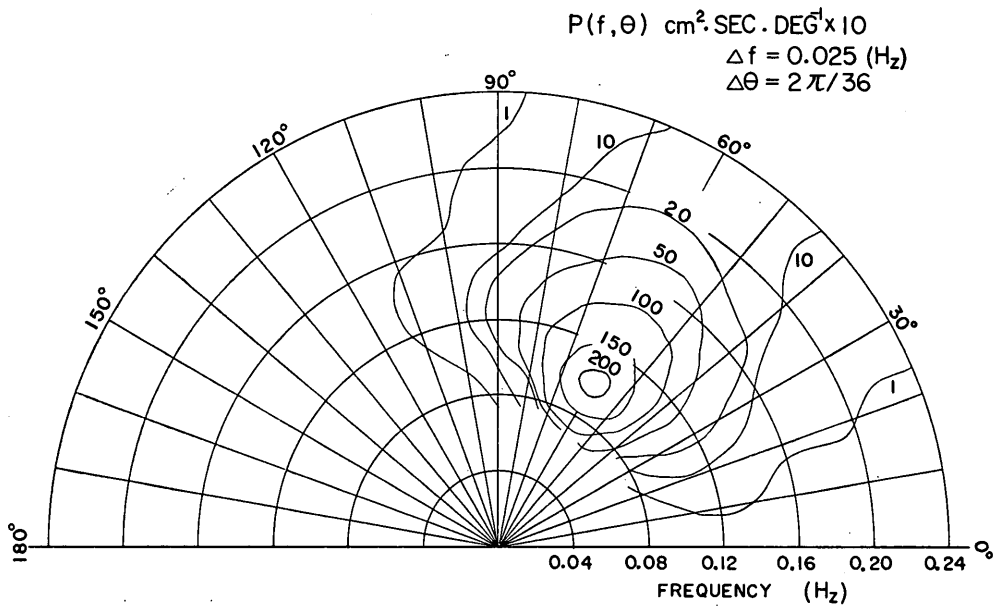


Fig. 20. Directional spectrum obtained from the linearized wave force

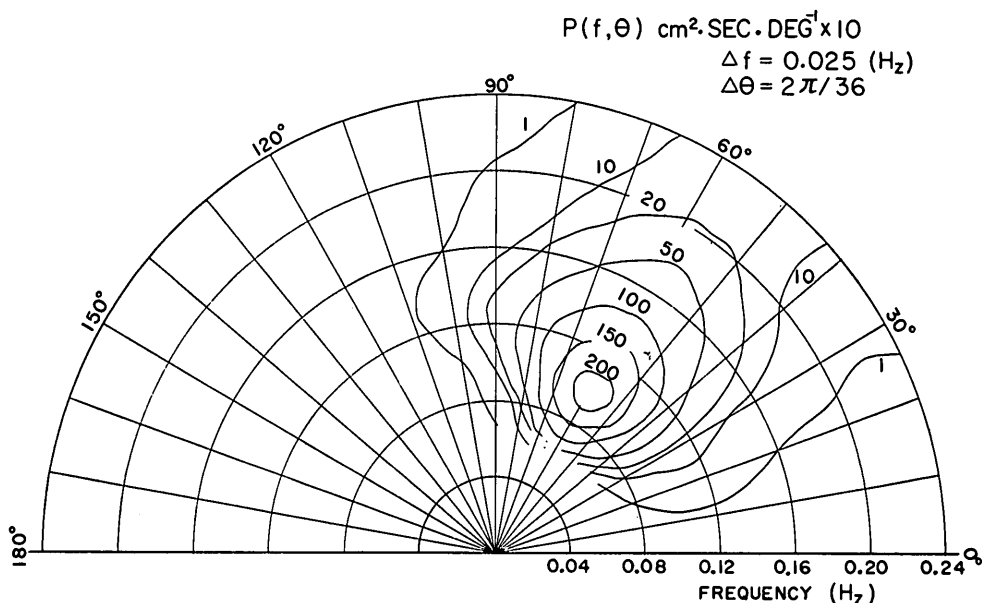


Fig. 21. Directional spectrum obtained from the non-linear wave force

For $3.75 \leq a < \infty$

$$\begin{aligned}
 a^{1/2}e^{-a}I_0(a) &= 0.39894228 + 0.01328592t^{-1} \\
 &+ 0.00225319t^{-2} - 0.00157565t^{-3} \\
 &+ 0.00916281t^{-4} - 0.02057706t^{-5} \\
 &+ 0.02635537t^{-6} - 0.01647633t^{-7} \\
 &+ 0.00392377t^{-8} + \epsilon \\
 |\epsilon| &< 1.9 \times 10^{-7}
 \end{aligned} \tag{129}$$

$$\begin{aligned}
 a^{1/2}e^{-a}I_1(a) &= 0.39894228 - 0.03988024t^{-1} \\
 &- 0.00362018t^{-2} + 0.00163801t^{-3} \\
 &- 0.01031555t^{-4} + 0.02282967t^{-5} \\
 &- 0.02895312t^{-6} + 0.01787654t^{-7} \\
 &- 0.00420059t^{-8} + \epsilon \\
 |\epsilon| &< 2.2 \times 10^{-7}
 \end{aligned} \tag{130}$$

where $t = a/3.75$

The following equation was used for obtaining higher order values.

$$I_{n+1}(a) = -\frac{2n}{a} I_n(a) + I_{n-1}(a) \tag{131}$$

5.5 Characteristics of the simulated data

The characteristics of the simulated data which were used in the previous section will be discussed here.

The histograms of η , η_p , V_x , V_y , A_x , A_y , F_x and F_y from the non-linear drag term for case 1-d or 2-b are shown in Fig. 22~31. The total number of data is 600

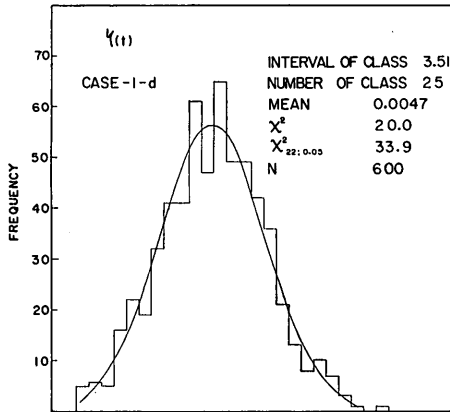


Fig. 22. Frequency histogram of simulated surface wave, $\eta(t)$, case 1-d

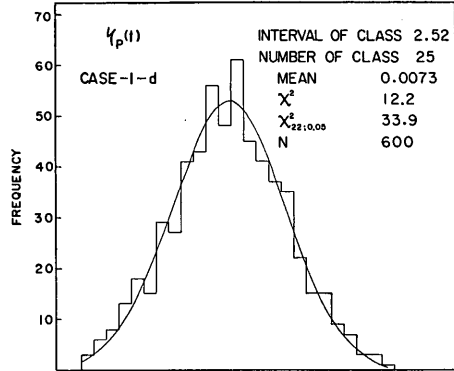


Fig. 23. Frequency histogram of simulated underwater pressure fluctuation, $\eta_p(t)$, case 1-d

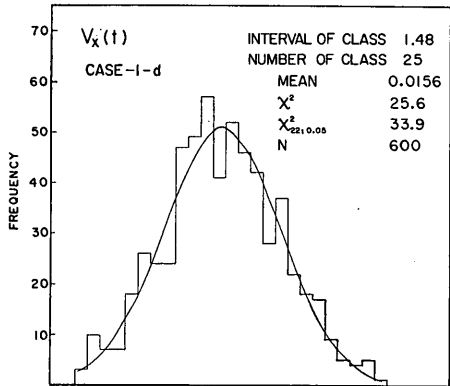


Fig. 24. Frequency histogram of simulated x component of water particle velocity, $V_x(t)$, case 1-d

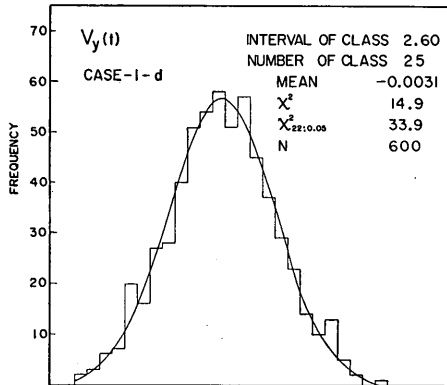


Fig. 25. Frequency histogram of simulated y component of water particle velocity, $V_y(t)$, case 1-d

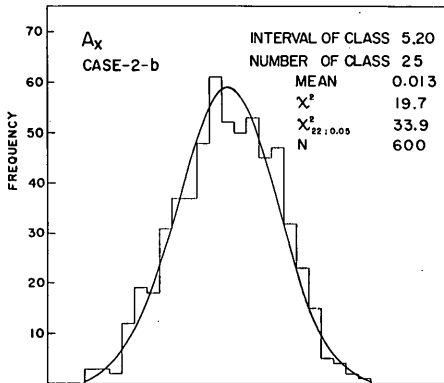


Fig. 26. Frequency histogram of simulated x component of water particle acceleration $A_x(t)$, case 2-b

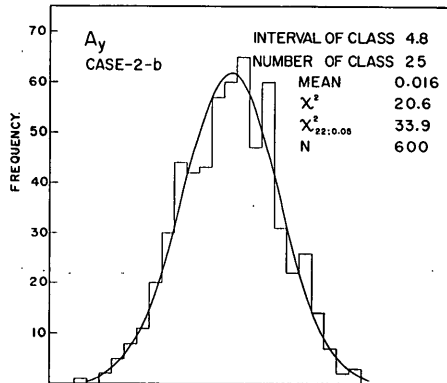


Fig. 27. Frequency histogram of simulated y component of water particle acceleration $A_y(t)$, case 2-b

Determination of Approximate Directional Spectra for Coastal Waves

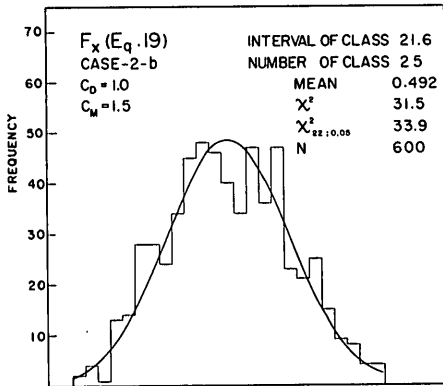


Fig. 28. Frequency histogram of simulated x component of linearized wave force, $F_x(t)$ (Eq. 19), case 2-b

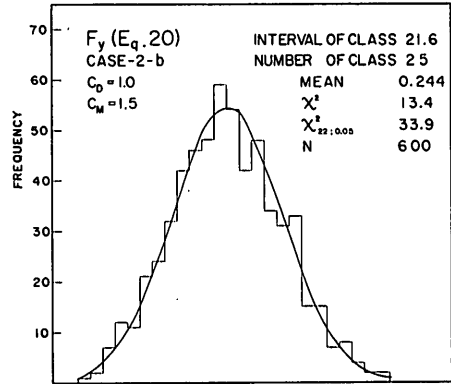


Fig. 29. Frequency histogram of simulated y component of linearized wave force, $F_y(t)$ (Eq. 20), case 2-b

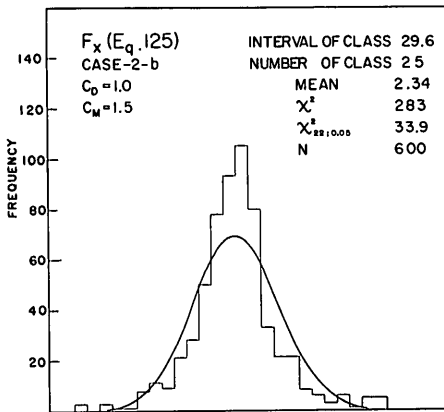


Fig. 30. Frequency histogram of simulated x component of non-linear wave force, $F_x(t)$ (Eq. 125), case 2-b

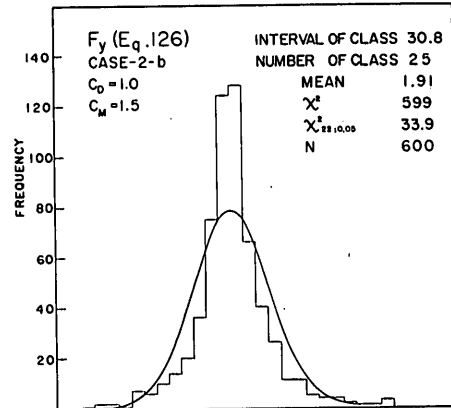


Fig. 31. Frequency histogram of simulated y component of non-linear wave force, $F_y(t)$ (Eq. 126), case 2-b

for each case. In these figures, the results of the Chi-square goodness-of-fit test are shown. For sample size 600 and the probability of a Type I Error of 5%, the minimum optimum number of class intervals is known¹⁹⁾ as 24. All wave properties, except F_x and F_y obtained from the non-linear drag term, have the Gaussian distribution. For the F_x and F_y from Eq. (125) and (126), the deviation from the Gaussian distribution becomes large when the A value in the Bretschneider-Pierson spectrum becomes large. However, their distribution approaches to the Gaussian distribution when C_M/C_D value becomes large. Since the simulated wave particle velocity and acceleration have the Gaussian distribution, it is natural that the F_x and F_y from the linearized drag term have the Gaussian distribution. The same can be said for the distribution properties of the other simulated data, case 2-b or case 1-d.

Power spectra for surface waves are shown in Fig. 32. In the Fig. 32, given power spectrum and power spectrum of case 1-a and of case 2-a are shown for

the convenience of comparison. The difference of the root-mean-square-value among them may be caused by the reduction of the range for the numerical integration. The root-mean-square value of case 1-*a* is larger than that of case 2-*a*. It is because the *a* value for case 1-*a* is larger than that of case 2-*a*.

6. Sample Calculation

6.1 Method of observation

In order to obtain the actual data for the wave properties, a pressure type wave meter and a strain-gauge type wave direction meter were used. The strain-gauge type wave direction meter has been developed by the Port and Harbour Research Institute, Ministry of Transport, Japan and has been used tentatively for the determination of wave direction at a point in shallow water.

The principle of the observation of the wave direction is as follows:

The apparatus consists of a transducer, conductor cable and a recording instrument. The schematic figure of the transducer is shown in Fig. 33. The rod, *R*, is bent by the wave force acting on the sphere. The strain at part *A* along the surface of the rod is measured by four wire strain-gauges attached on the rod as shown in Fig. 34. The four wire strain-gauges compose a bridge circuit, and detect the magnitude of the *x* and *y* component of the wave force. The resultant direction of the wave force can be determined by the instantaneous value of *x* and *y* component of the wave force.

In order to obtain the wave direction for the surface wave, it is assumed

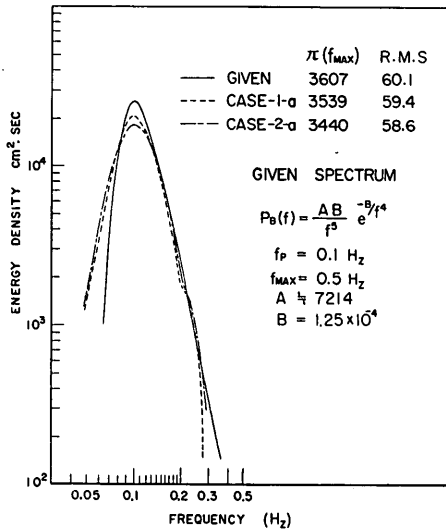


Fig. 32. Comparison of power spectrum
Given spectra, case 1-*a* and case 2-*a*

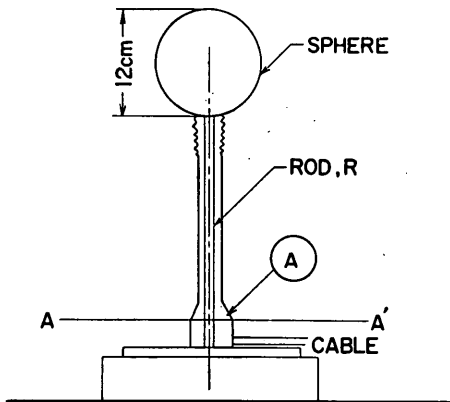


Fig. 33. Schematic figure of the wave direction meter

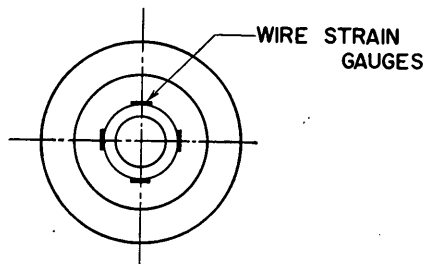


Fig. 34. Section A-A'

Determination of Approximate Directional Spectra for Coastal Waves

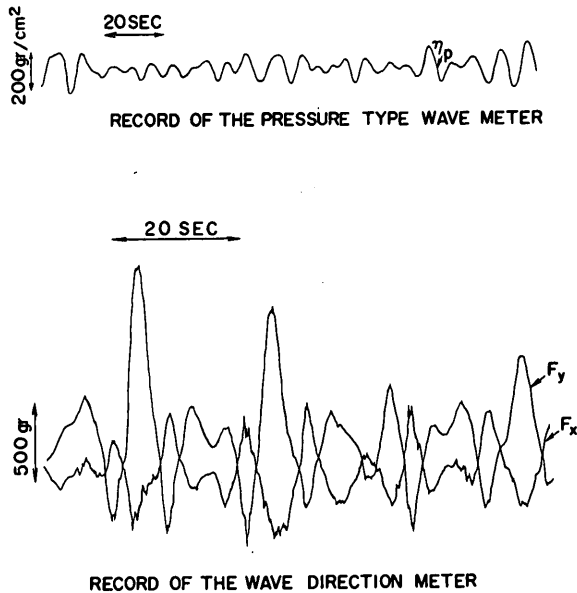


Fig. 35. Example of the record obtained at SAKATA

conventionally that the resultant wave force direction coincides with the direction of the surface wave. Examples of the records taken by the instrument as well as the one by the wave meter are shown in Fig. 35. These data were taken at Sakata Port along the Japan Sea Coast in the northern part of Japan, and the geographic relations for the instruments are shown in Fig. 36.

6.2 Results of calculation

The data which were used here had been taken at Sakata Port during 15.50~16.00 on November 14, 1966. The maximum lag time was chosen to be 24.5 seconds. This results in the degree of freedom being about 50. The distance between the wave meter and the wave direction meter was assumed to be zero.

The power spectrum of η_p, F_x, F_y are shown in Fig. 37. The co- and quadratur-spectra for η_p, F_x and η_p, F_y and F_x, F_y are shown in Fig. 38~40. The values C_D and C_V were calculated by the relation given by Eq. (101) and Eq. (102). These values are plotted in Fig. 41.

The values a and γ were obtained by Eq. (80) to Eq. (89) replaced by C_D''', C_M''' , and η_p instead of $C_D'', C_M'',$ and η , respectively. The ratio of the modified Bessel function of the first kind, $I_0(a)/I_2(a)$, and a value are shown in Fig. 42 as well as

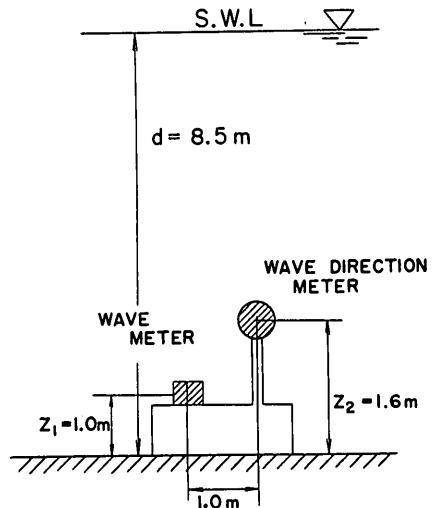


Fig. 36. Geographic relation between the wave meter and the wave direction meter installed at SAKATA

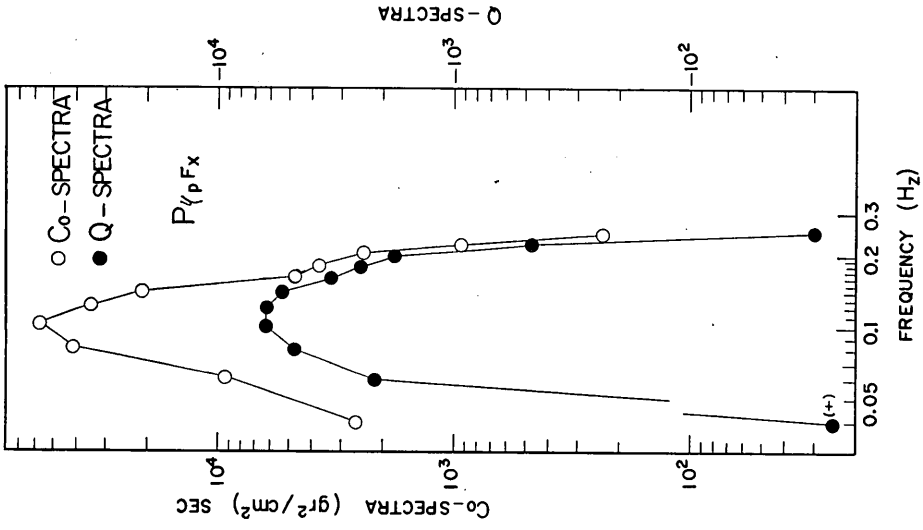


Fig. 38. Co- and quadrature-spectra of pressure fluctuation and x component of wave force at SAKATA

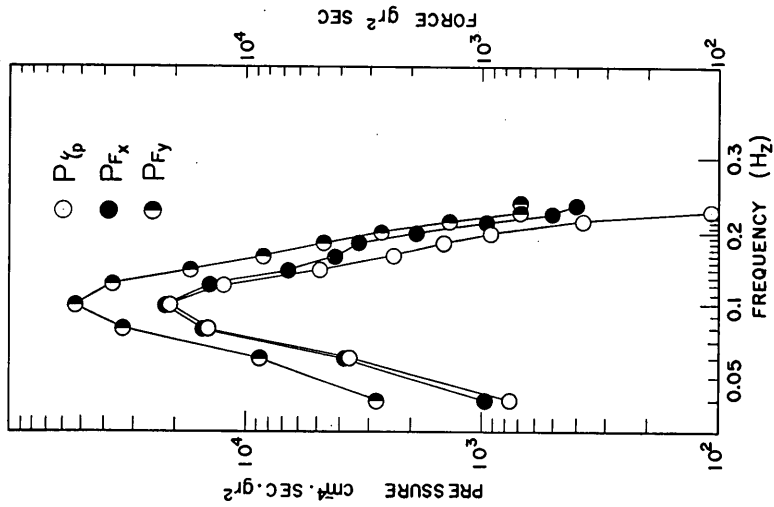


Fig. 37. Power spectra of pressure fluctuation, x component of wave force, and y component of wave force at SAKATA

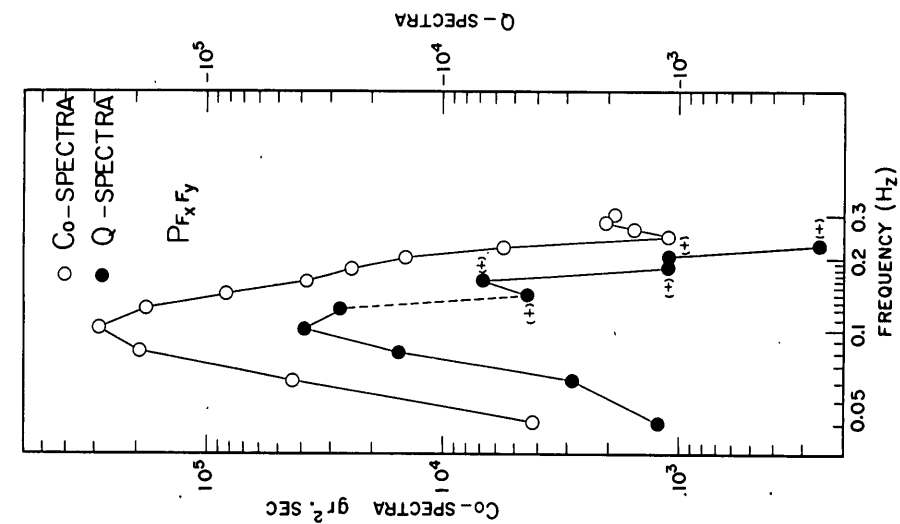


Fig. 39. Co- and quadrature-spectra of pressure fluctuation and y component of wave force at SAKATA

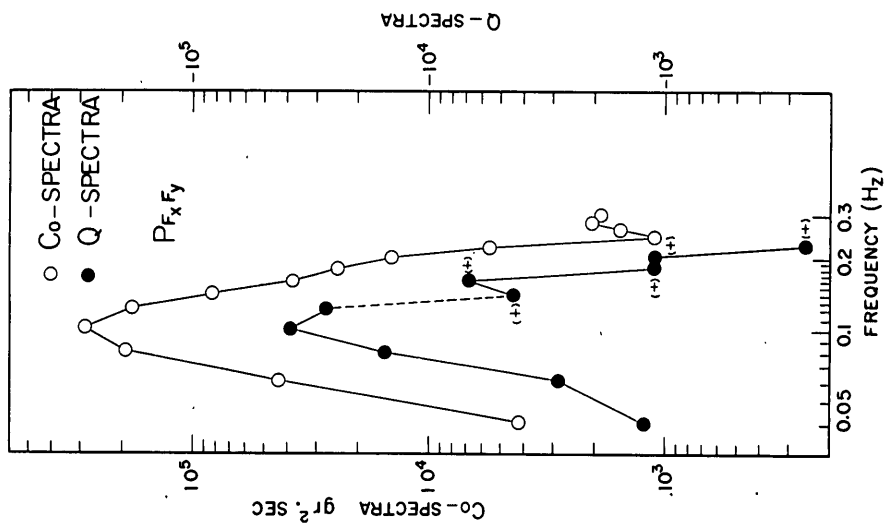


Fig. 40. Co- and quadrature-spectra of x and y component wave force at SAKATA

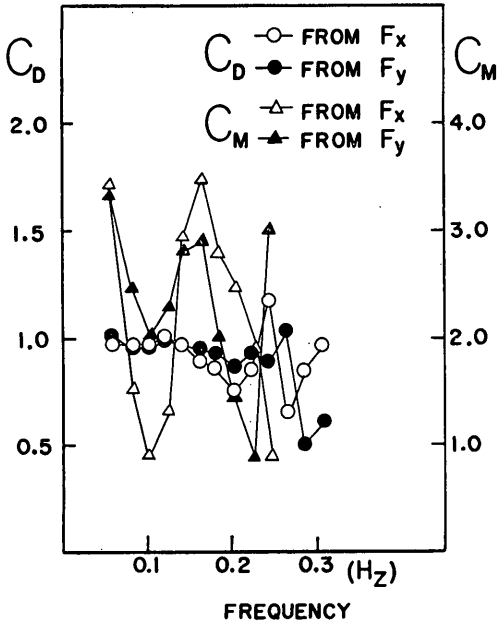


Fig. 41. C_D and C_M obtained in the sample calculation

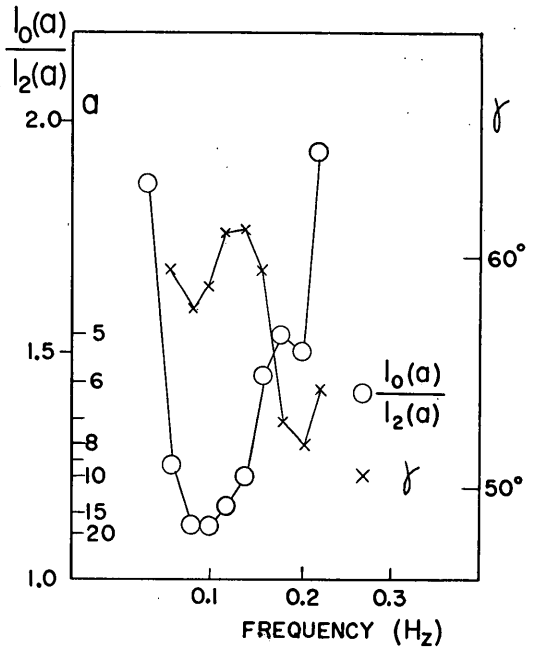


Fig. 42. $I_0(a)/I_2(a)$ and γ vs ω obtained in the sample calculation

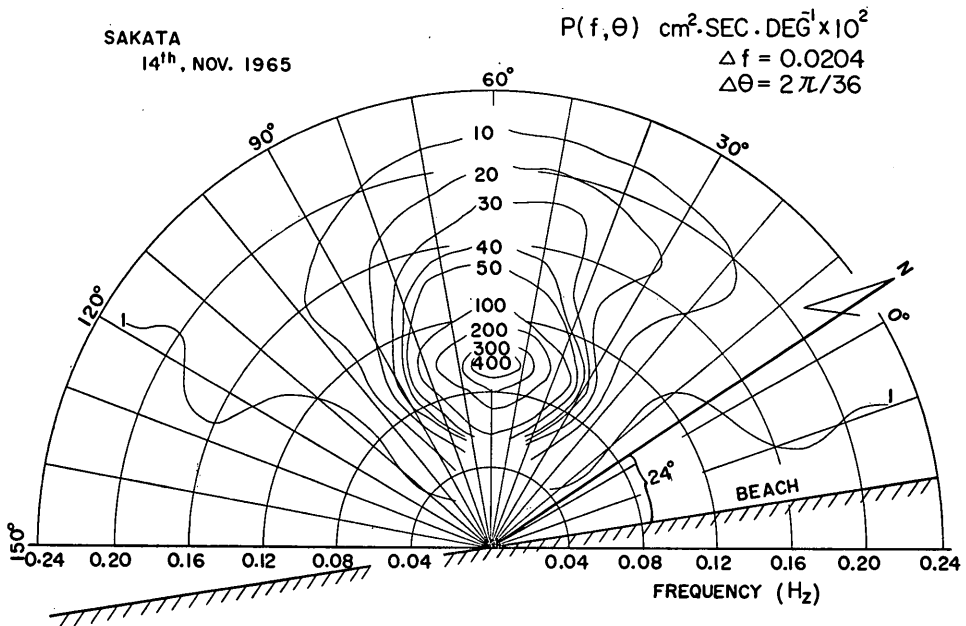


Fig. 43. Directional spectra obtained in the sample calculation

γ value obtained by Eq. (81). Fig. 43 shows the directional spectra which were calculated by the a and γ value.

7. Discussion

There exist some ambiguities in the method although some results have been obtained. First of all, the assumption that the conventional wave force formula can be expressed by Eq. (18) should be discussed. The results from section 5 where the accuracy of the method was discussed, show that the linear-approximation does not affect much the estimation of γ and C_D and C_M values. The a value, however, is affected by the linear approximation very much. Since the small change of $I_0(a)/I_3(a)$ causes significant change of a value, the accuracy of the spectral analysis might have some effects on the estimation of a value.

As shown in section 5.5, the distribution of F_x and F_y obtained from Eqs. (125) and (126) deviate from the Gaussian distribution for large A and relatively small C_M/C_D . This means that the assumption of the Gaussian distribution for the force component does not hold when the amount of wave energy is large and C_M/C_D is small.

The results from the sample calculation show that $C_M \doteq 1.5$ and $C_D \doteq 1.0$ around the peak frequency of energy spectra (0.1 Hz). The value C_M is very close to the theoretical one and C_D may be reasonable. This means that the actual wave force may not have the Gaussian distribution. The distribution of the component wave force of the actual data which were analyzed as an example is shown in Fig. 44 and 45. Both distribution are not the Gaussian distribution. Since the restriction mentioned above is inevitable, the value a would be estimated well provided that the A value is small. For examining the accuracy of the example

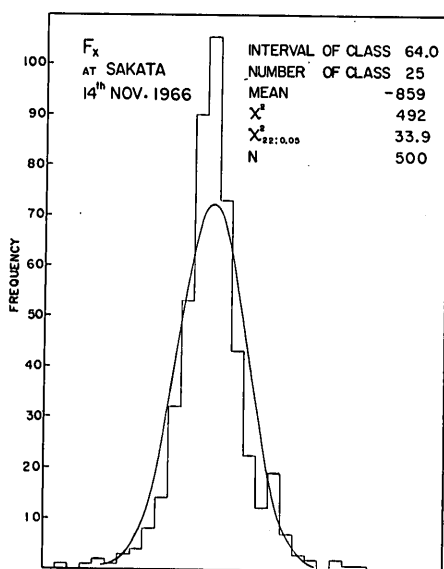


Fig. 44. Frequency histogram of x component wave force observed at SAKATA

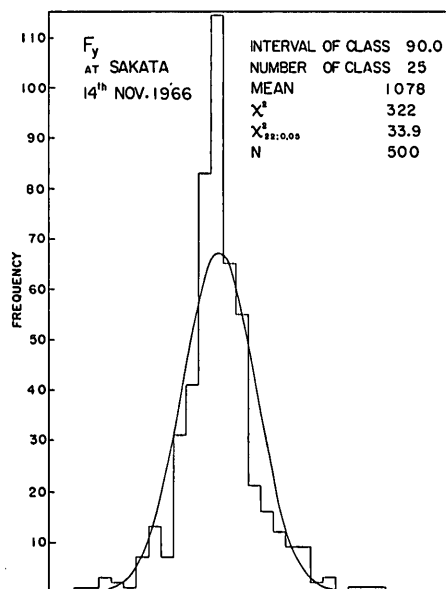


Fig. 45. Frequency histogram of y component wave force observed at SAKATA

calculation, small a value like 8~12 should have been used. Further investigation of the accuracy is remained.

In the example calculation, C_D was about 1.0 and C_M was about 1.5. These values, however, change magnitude considerably as frequency changes. Especially, for the higher frequency, the values reached are three times or more larger than that at the peak frequency. Since the obtained power spectrum densities have less accuracy in higher frequency, the facts mentioned above might not explain that C_D and C_M value change remarkably for higher frequency.

The directional spectra which were used for generating the simulated wave properties are considered to be special cases such that they had one peak in frequency and in azimuth. Various other cases should be investigated to clear the accuracy of the method. The results of field observation will give us fruitful information on the use of the method.

8. Conclusion

1) This method can be applied for the determination of the approximate directional spectra of sea waves at one location, if the instrument be suitably installed so that the distance between the wave meter and the wave direction meter are considered to be zero compared with the wave length.

2) This method is very useful for the investigation of the wave direction at which main wave energy is advancing. Indeed, the procedure should prove useful for the investigation of the directions of the waves from several storms, provided there is a frequency difference between the energy associated with each of the storms.

3) The value C_D and C_M can be estimated by this method as a function of frequency.

4) Other advantages may be that:

a) By the method, long term, continuous, and all-weather wave direction observation would be secured,

b) The observation cost may be cheaper than any other method.

Acknowledgement

The author wishes to express his deepest appreciation to professor L. E. Borgman at the Univ. of California, Berkeley. He suggested the method of derivation and offered help and criticism for which the author is very grateful. The author also wishes to express his thanks to Dr. T. Hamada whose criticism enabled the author to accomplish this study.

Expression of indebtedness is also due to Chief T. Takahashi, Mr. H. Sasaki, and the rest of the staff of the Inquiry and Investigation Section, Hydraulics Division, Port and Harbour Research Institute, for permitting the author to analyze the actual data taken at Sakata Port, and for encouraging the author. Figures are made by Mr. T. Nakai.

Reference

- 1) Cummins, W.E.: "The Determination of Directional Wave Spectra in the TMB Maneuvering-Seakeeping Basin," *12th American Towing Tank Conference at U.C. Berkely*,

Determination of Approximate Directional Spectra for Coastal Waves

- Report 1362, September 1959.
- 2) Barber, N.F.: "The Directional Resolving Power of an Array of Wave Detectors," *Conference on Ocean Wave Spectra*, 1961.
 - 3) Mobarek, I.E.: "Directional Spectra of Laboratory Wind Waves," *Proc. of A.S.C.E. WW3*, 1965.
 - 4) Cote, L.J., et. al.: "The Directional Spectrum of a Wind Generated Sea as Determined from Data Obtained by the Stereo Wave Observation Project," *N.Y. Univ., Dept. of Meteorology and Oceanography*, 1957.
 - 5) Ijima, T. and T. Matsuo: "Study on waves in surf zone" *Proc. 15th conf. on Coastal Eng. in Japan*, 1968. (in Japanese)
 - 6) Longuet-Higgins, M.S. and D.E. Cartwright: "Observation of the Directional Spectrum of Sea Waves Using the Motion of a Floating Buoy," *Conference on Ocean Wave Spectra*, 1961.
 - 7) Ewing, J.A.: "Some Measurement of the Directional Wave Spectrum" *Jour. of Marine Research*, Vol. 27, No. 2, 1969.
 - 8) Nagata, Y.: "The Statistical Properties of Orbital Wave Motions and Their Application for the Measurement of Directional Wave Spectra," *Journal of the Oceanographical Society of Japan*, Vol. 19, No. 4, 1964.
 - 9) Lamb, H.: "Hydrodynamics," *Dover Publication*, 1945.
 - 10) Pierson, W.J., Jr.: "The Representation of Ocean Surface Waves by a Three-Dimensional Stationary Gaussian Process," N.Y. Univ., 1954; Kinsman, B., "Wind Waves," Prentice-Hall, 1965.
 - 11) Pierson, W.J.: "Method for the Time Series Analysis of Water Wave Effects on Piles," *TN-479, U.S. Navy Civil Eng. Lab.*, Port Hueneme, California, (1963).
 - 12) Pierson, W.J., Jr. and P. Holmes: "The Force on a Pile Due to Irregular Waves," *Proc. of A.S.C.E. WW4*, 1965.
 - 13) Borgman, L.E.: "Random Hydraulic Forces on Objects," *The Annals of Mathematical Statistics*, Vol. 38, No. 1, 1967.
 - 14) Brown, J.L. and L.E. Borgman: "Table of the Statistical Distribution of Ocean Wave Forces and Methods for the Estimation of C_D and C_M " *HEL 9-7, U.C. Berkeley*, 1966.
 - 15) Wiegel, R.L.: "Oceanographical Engineering," *Prentice-Hall*, 1964.
 - 16) Borgman, L.E.: "Ocean Wave Simulation for Engineering Design," *HEL 9-13, U.C. Berkeley*, 1967.
 - 17) Gumbel, E.J.: "The Circular Normal Distribution," *Journal of American Statistical Association*, Vol. 48, 1953.
 - 18) Court, A.: "Some New Statistical Techniques in Geophysics," *Advances in Geophysics*, Vol. 1, 1952.
 - 19) Bendat, J.S. and A.G. Piersol: "Measurement and Analysis of Random Data", *John Wiley & Sons, Inc*, 1966.
 - 20) Abramowitz, M. and I.A. Stegun: "Handbook of Mathematical Functions with Formulas, Graphs, and Mathematical Tables" *U.S. Department of Commerce, National Bureau of Standards*, Applied Mathematics Series No. 55, 1964.
 - 21) Suzuki, Y.: "Determination of Approximate Directional Spectra for Surface Waves," *Hydraulic Engr. Lab. Rep. HEL 1-11, U.C. Berkeley*, 1968.

List of Symbols

- A : constant in the Bretschneider-Pierson spectrum
 A_c : water particle acceleration
 A_x : x component of water particle acceleration
 A_y : y component of water particle acceleration
 $A_x(x, y, z; t)$: pseudo-integral representation for x component of water particle acceleration at space-point (x, y, z) and time t
 $A_y(x, y, z; t)$: pseudo-integral representation for y component of water particle acceleration at space-point (x, y, z) and time t
 $A'_x(x, y, z; t)$: simulated x component of water particle acceleration at space-point (x, y, z) and time t
 $A'_y(x, y, z; t)$: simulated y component of water particle acceleration at space-point (x, y, z) and time t
 a : constant, a measure of the concentration around the mean
 B : constant in the Bretschneider-Pierson spectrum
 C : coefficient for drag term (Eq. 17)
 C_1 : coefficient for drag term (Eq. 15)
 C_2 : coefficient for inertial term (Eq. 15)
 C_D : drag coefficient
 C''_D : parameter related to drag coefficient (Eq. 29, for surface wave)
 C'''_D : parameter related to drag coefficient (Eq. 92, for underwater pressure fluctuation)
 C'''_{DX} : C'''_D calculated from x component terms
 C'''_{DY} : C'''_D calculated from y component terms
 C_M : inertial coefficient
 C''_M : parameter related to inertial coefficient (Eq. 30, for surface wave)
 C'''_M : parameter related to inertial coefficient (Eq. 93, for underwater pressure fluctuation)
 C'''_{MX} : C'''_M calculated from x component terms
 C'''_{MY} : C'''_M calculated from y component terms
 $C_{F_x F_x}(g, h, \tau)$: cross-covariance between $F_x(x, y, z; t)$ and $F_x(x+g, y+h, z; t+\tau)$
 $C_{F_x F_y}(g, h, \tau)$: cross-covariance between $F_x(x, y, z; t)$ and $F_y(x+g, y+h, z; t+\tau)$
 $C_{F_y F_y}(g, h, \tau)$: cross-covariance between $F_y(x, y, z; t)$ and $F_y(x+g, y+h, z; t+\tau)$
 $C_{\eta F_x}(g, h, \tau)$: cross-covariance between $\eta(x, y; t)$ and $F_x(x+g, y+h, z; t+\tau)$
 $C_{\eta F_y}(g, h, \tau)$: cross-covariance between $\eta(x, y; t)$ and $F_y(x+g, y+h, z; t+\tau)$
 $C_{\eta\eta}(g, h, \tau)$: cross-covariance between $\eta(x, y; t)$ and $\eta(x+g, y+h; t+\tau)$
 $C_{\eta\eta(m,n)}(g, h, \tau)$: cross-covariance of the (m, n) th term in the sum in Eq. (1)
 $co(f)$: co-spectral density of $X_1(t)$ and $X_2(t)$
 $co_{F_x F_x}(f)$: co-spectral density of $F_x(x, y, z; t)$ and $F_x(x+g, y+h, z; t)$
 $co_{F_x F_y}(f)$: co-spectral density of $F_x(x, y, z; t)$ and $F_y(x+g, y+h, z; t)$
 $co_{F_y F_y}(f)$: co-spectral density of $F_y(x, y, z; t)$ and $F_y(x+g, y+h, z; t)$
 $co_{\eta F_x}(f)$: co-spectral density of $\eta(x, y; t)$ and $F_x(x+g, y+h, z; t)$
 $co_{\eta F_y}(f)$: co-spectral density of $\eta(x, y; t)$ and $F_y(x+g, y+h, z; t)$
 $co_{\eta\eta}(f)$: co-spectral density of $\eta(x, y; t)$ and $\eta(x+g, y+h, t)$
 $\hat{co}_{F_x F_x}(f)$: co-spectral density of $F_x(t)$ and $F_x(t)$
 $= P_{F_x}(f)$, power spectral density of $F_x(t)$
 $\hat{co}_{F_x F_y}(f)$: co-spectral density of $F_x(t)$ and $F_y(t)$

Determination of Approximate Directional Spectra for Coastal Waves

- $\hat{c}o_{F_y F_y}(f)$: co-spectral density of $F_y(t)$ and $F_y(t)$
 $= P_{F_y}(f)$, power spectral density of $F_y(t)$
- $\hat{c}o_{\eta F_x}(f)$: co-spectral density of $\eta(t)$ and $F_x(t)$
- $\hat{c}o_{\eta F_y}(f)$: co-spectral density of $\eta(t)$ and $F_y(t)$
- $\hat{c}o_{\eta \eta}(f)$: co-spectral density of $\eta(t)$ and $\eta(t)$
 $= P_{\eta}(f)$, power spectral density of $\eta(t)$
- $C_{X_1 X_2}(\tau)$: cross-covariance between $X_1(t)$ and $X_2(t)$
- $C_{X_1 X_2}(g, h, \tau)$: cross-covariance between $X_1(x, y, t)$ and $X_2(x+g, y+h, t+\tau)$
- D : horizontal distance between wave meter and wave direction meter
- d : depth of water at the installation point
- F : wave force, unidirectional case
- F_x : x component of wave force F
- F_y : y component of wave force F
- $F_x(x, y, z, t)$: x component wave force at space-point (x, y, z) and time t (with directional spectrum)
- $F_y(x, y, z, t)$: y component wave force at space-point (x, y, z) and time t (with directional spectrum)
- f : frequency (Hz)
- f_m : frequency defined by Eq. 6.
- f_{MAX} : frequency at which energy density of the power spectrum can be assumed to be zero
- f_p : frequency at which energy density of the power spectrum becomes largest value
- G : constant, see Eq. 122
- g : acceleration of gravity, also space lag in x axis
- h : space lag in y axis
- $h(\theta)$: probability density of the circular normal distribution
- $I_n(a)$: modified Bessel Function of 1st kind, order n
- $J_p(kD)$: Bessel Function of 1st kind
- K : constant for generating of the pseudo-random numbers
- K_D : constant $= (C_{D\omega}/2g)\pi r^2 C$
- K_M : constant $= (C_{M\omega}/g)(4/3)\pi r^3$
- k : wave number
- k_m : wave number for the wave with the frequency of f_m at the water depth of d
- $L(a, \gamma)$: see Eq. 64
- $L'(a, \gamma)$: see Eq. 65
- M : numbers of subdivisions in frequency
- M_0 : constant for generating of the pseudo-random numbers
- m : subscript referring to frequency
- N : numbers of subdivisions in azimuth
- n : subscript referring to azimuth, also integer for $I_n(a)$, $J_n(KD)$, X_n
- p : subscript referring to underwater pressure fluctuation, also integer
- $p(f, \theta)$: directional spectral density
- $p_B(f)$: Bretschneider-Pierson spectral density
- $P_{F_x}(f)$: power spectral density of $F_x(t)$, $= \hat{P}_{F_x F_x}(f) = \hat{c}o_{F_x F_x}(f)$
- $P_{F_x F_x}(f)$: cross-spectral density of $F_x(x, y, t)$ and $F_x(x+g, y+h, t)$
- $P_{F_x F_y}(f)$: cross-spectral density of $F_x(x, y, t)$ and $F_y(x+g, y+h, t)$
- $P_{F_y}(f)$: power spectral density of $F_y(t)$, $= \hat{P}_{F_y F_y}(f) = \hat{c}o_{F_y F_y}(f)$

- $P_{F_y F_y}(f)$: cross-spectral density of $F_y(x, y, t)$ and $F_y(x+g, y+h, t)$
 $P_\eta(f)$: power spectral density of $\eta(t)$, $=\hat{P}_{\eta\eta}(f)=\hat{c}\hat{o}_{\eta\eta}(f)$
 $\eta_{\eta F_x}(f)$: cross-spectral density of $\eta(x, y, t)$ and $F_x(x+g, y+h, t)$
 $P_{\eta F_y}(f)$: cross-spectral density of $\eta(x, y, t)$ and $F_y(x+g, y+h, t)$
 $P_{\eta\eta}(f)$: power spectral density of $\eta(f)$
 $P_{\eta\eta}(f)$: cross-spectral density of $\eta(x, y, t)$ and $\eta(x+g, y+h, t)$
 $P_V(f)$: power spectral density of water particle velocity
 $P_{X_1 X_2}(f)$: cross-spectral density of $X_1(t)$ and $X_2(t)$
 $\hat{P}_{F_x F_x}(f)$: cross-spectral density of $F_x(t)$ and $F_x(t)$
 $=P_{F_x}(f)$, power spectral density of $F_x(t)$
 $\hat{P}_{F_x F_y}(f)$: cross-spectral density of $F_x(t)$ and $F_y(t)$
 $\hat{P}_{F_y F_y}(f)$: cross-spectral density of $F_y(t)$ and $F_y(t)$
 $=P_{F_y}(f)$, power spectral density of $F_y(t)$
 $\hat{P}_{\eta F_x}(f)$: cross-spectral density of $\eta(t)$ and $F_x(t)$
 $\hat{P}_{\eta F_y}(f)$: cross-spectral density of $\eta(t)$ and $F_y(t)$
 $\hat{P}_{\eta\eta}(f)$: cross-spectral of $\eta(t)$ and $\eta(t)$
 $=P_\eta(f)$, power spectral density of $\eta(t)$
 Q : maximum frequency (Eq. 1)
 $q(f)$: q -spectral density of $X_1(t)$ and $X_2(t)$
 $q_{F_x F_x}(f)$: q -spectral density of $F_x(x, y, z; t)$ and $F_x(x+g, y+h, z; t)$
 $q_{F_y F_y}(f)$: q -spectral density of $F_y(x, y, z; t)$ and $F_y(x+g, y+h, z; t)$
 $q_{\eta F_x}(f)$: q -spectral density of $\eta(x, y; t)$ and $F_x(x+g, y+h, z; t)$
 $q_{\eta F_y}(f)$: q -spectral density of $\eta(x, y; t)$ and $F_y(x+g, y+h, z; t)$
 $q_{\eta\eta}(f)$: q -spectral density of $\eta(x, y; t)$ and $\eta(x+g, y+h, t)$
 $\hat{q}_{\eta F_x}(f)$: q -spectral density of $\eta(t)$ and $F_x(t)$
 $\hat{q}_{\eta F_y}(f)$: q -spectral density of $\eta(t)$ and $F_y(t)$
 r : radius of the sphere
 $S(f, \theta)$: cumulative spectrum of $p(f, \theta)$
 t : time, also $=a/3.75$ (Eq. 129, 130)
 V : water particle velocity, unidirectional case
 V_{rms} : root-mean-square value of V
 V_x : x component of V
 V_y : y component of V
 $V_x(x, y, z, t)$: x component of water particle velocity at space-point (x, y, z) and time t (with directional spectrum)
 $V_y(x, y, z, t)$: y component of water particle velocity at space-point (x, y, z) and time t (with directional spectrum)
 $V'_x(x, y, z, t)$: simulated x component of water particle velocity at space-point (x, y, z) and time t
 $V'_y(x, y, z, t)$: simulated y component of water particle velocity at space-point (x, y, z) and time t
 X_0 : initial value for generating of the pseudo-random numbers by congruence method
 $X_1(t)$: time series, real Gaussian stationary processes
 $X_2(t)$: time series, real Gaussian stationary processes
 $X_i(x, y, t)$: time series with the parameters, x, y and t , real Gaussian stationary processes

Determination of Approximate Directional Spectra for Coastal Waves

- $X_1(x, y, t)$: time series with the parameters, x, y and t , real Gaussian stationary processes
- X_n : pseudo-random numbers
- $\{X_n\}$: sequence of pseudo-random numbers
- x : subscript referring to x component
- y : subscript referring to y component
- z : subscript referring to vertical component
- z_1 : installation depth of wave measured from the bottom
- z_2 : installation depth of wave direction meter measured from the bottom
- α : parameter ($=\theta-\gamma$)
- β : angle between x axis and the line on which wave meter and wave direction meter lie
- γ : constant angle at which the maximum energy of waves is advancing
- ε : error in calculating the modified Bessel Function of 1st kind by Eqs. 129, 130
- η : subscript referring to sea surface
- $\eta(x, y, t)$: pseudo-integral representation for sea surface at space-point (x, y) and time t
- $\hat{\eta}(x, y, t)$: Pierson's representation for sea surface at space-point (x, y) and time t
- $\eta'(x, y, t)$: simulated sea surface at space-point (x, y) and time t
- $\eta_p(x, y, z; t)$: pseudo-integral representation for underwater pressure fluctuation at space-point (x, y, z) and time t
- $\eta'_p(x, y, z; t)$: simulated underwater pressure fluctuation at space-point (x, y, z) and time t
- θ : direction of wave advancing
- θ_n : direction of wave advancing defined by Eq. 7
- λ : parameter ($=\alpha+\gamma-\beta$)
- $H(f)$: cumulative spectrum of $p(f, \theta)$ at $\theta=2\pi$
- π : constant (3.14159.....)
- τ : lag in time
- Φ : random phase
- Φ_{mn} : random phase for each wavelet
- Φ_n : pseudo-random phase
- φ : constant
- ω : specific weight of sea water

Determination of Approximate Directional Spectra for Coastal Waves

Table with 7 columns: NO, WAVE(S), WAVE(P), X-VELOCITY, Y-VELOCITY, X-ACCEL, Y-ACCEL. Contains 38 data rows (NO 301-400).

Table with 7 columns: NO, WAVE(S), WAVE(P), X-VELOCITY, Y-VELOCITY, X-ACCEL, Y-ACCEL. Contains 38 data rows (NO 351-400).

